Exelon Generation®

200 Exelon Way
Kennett Square, PA 19348

www.exeloncorp.com

PROPRIETARY INFORMATION – WITHHOLD UNDER 10 CFR 2.390

10 CFR 50.55a

November 24, 2020

U.S. Nuclear Regulatory Commission
Attn: Document Control Desk
Washington, DC 20555-0001

Peach Bottom Atomic Power Station, Unit 2
Renewed Facility Operating License No. DPR-44
NRC Docket No. 50-277

Subject: Relief Request Associated with N-16A Reactor Pressure Vessel Instrument Nozzle Repairs – Submittal of Analyses

References:

1. Letter from D. P. Helker (Exelon Generation Company, LLC) to U.S. Nuclear Regulatory Commission, "Proposed Relief Request Associated with N-16A Reactor Pressure Vessel Instrument Nozzle Repairs," dated November 4, 2020 (ML20309B020)

2. Email from J. Tobin (U.S. Nuclear Regulatory Commission) to D. Helker (Exelon Generation Company, LLC), "Peach Bottom Verbal Relief for Penetration Nozzle (EPID: L-2020-LLR-0144)," dated November 6, 2020 (ML20314A028)

In Reference 1, in accordance with 10 CFR 50.55a, Exelon Generation Company, LLC (EGC) requested approval of a relief request associated with the repair of a 2-inch instrument line nozzle at penetration N-16A on the Reactor Pressure Vessel (RPV). Reference 2 provided the U.S. Nuclear Regulatory Commission (NRC) verbal authorization of the repair.

As discussed in Reference 1, EGC committed to supplying the final one-cycle flaw analytical evaluation, evaluation of repair, and the corrosion evaluation. Attached are these analyses.

Attachments 1 (“Peach Bottom 2 N16A Instrument Nozzle Repair J-Groove One-Cycle Justification,” Document Number 32-9321034-002), 2 (“Peach Bottom 2 N16A Instrument Nozzle Repair Stress One-Cycle Justification,” Document Number 32-9321033-003), and 3 (“Corrosion Evaluation of the Peach Bottom Unit 2 N16-A Reactor Vessel Nozzle Modification,” Document Number 51-9320932–001) contain information proprietary to Framatome Inc. (Framatome). Framatome requests that these documents be withheld from public disclosure in accordance with 10 CFR 2.390(a)(4). An affidavit supporting this request is contained in Attachment 4. Attachments 5, 6, and 7 contain non-proprietary versions of the Framatome documents.

Attachments 1, 2 and 3 contain proprietary information – the balance of this letter is considered non-proprietary when Attachments 1, 2 and 3 are removed.

If you have any questions or require additional information, please contact Tom Loomis at 610-765-5510.

Sincerely,

David P. Helker
Sr. Manager - Licensing
Exelon Generation Company, LLC

Attachments: 1) "Peach Bottom 2 N16A Instrument Nozzle Repair J-Groove One-Cycle Justification," Document Number 32-9321034-002 (Proprietary Version)

2) "Peach Bottom 2 N16A Instrument Nozzle Repair Stress One-Cycle Justification," Document Number 32-9321033-003 (Proprietary Version)

3) "Corrosion Evaluation of the Peach Bottom Unit 2 N16-A Reactor Vessel Nozzle Modification," Document Number 51-9320932–001 (Proprietary Version)

4) Affidavit

5) "Peach Bottom 2 N16A Instrument Nozzle Repair J-Groove One-Cycle Justification Non-Proprietary," Document Number 32-9321037–001 (Non-Proprietary Version)

6) "Peach Bottom 2 N16A Instrument Nozzle Repair Stress One-Cycle Justification Non-Proprietary," Document Number 32- 9321035–001 (Non-Proprietary Version)

7) "Corrosion Evaluation of the Peach Bottom Unit 2 N16-A Reactor Vessel Nozzle Modification," Document Number 51-9321006–001 (Non-Proprietary Version)

cc: USNRC Region I, Regional Administrator
USNRC Senior Resident Inspector, PBAPS
USNRC Project Manager, PBAPS
W. DeHass, Pennsylvania Bureau of Radiation Protection

Attachment 4

Affidavit

A F F I D A V I T

1. My name is Philip A. Opsal. I am Manager, Product Licensing for Framatome Inc. (formally known as AREVA Inc.), and as such I am authorized to execute this Affidavit.

2. I am familiar with the criteria applied by Framatome to determine whether certain Framatome information is proprietary. I am familiar with the policies established by Framatome to ensure the proper application of these criteria.

3. I am familiar with the Framatome information contained in the following Reports referred to herein as "Documents.":

- Framatome Engineering Information Record 51-9320932-001, "Corrosion Evaluation of the Peach Bottom Unit 2 N16-A Reactor Vessel Nozzle Modification," November 2020
- Framatome Calculation Summary Sheet (CSS) 32-9321033-003, "Peach Bottom 2 N16A Instrument Nozzle Repair Stress One-Cycle Justification," November 2020
- Framatome Calculation Summary Sheet (CSS) 32-9321034-002, "Peach Bottom 2 N16A Instrument Nozzle Repair J-Groove One-Cycle Justification," November 2020

Information contained in these Documents has been classified by Framatome as proprietary in accordance with the policies established by Framatome for the control and protection of proprietary and confidential information.

4. These Documents contain information of a proprietary and confidential nature and is of the type customarily held in confidence by Framatome and not made available to the

public. Based on my experience, I am aware that other companies regard information of the kind contained in these Documents as proprietary and confidential.

5. These Documents have been made available to the U.S. Nuclear Regulatory Commission in confidence with the request that the information contained in these Documents be withheld from public disclosure. The request for withholding of proprietary information is made in accordance with 10 CFR 2.390. The information for which withholding from disclosure is requested qualifies under 10 CFR 2.390(a)(4) “Trade secrets and commercial or financial information.”

6. The following criteria are customarily applied by Framatome to determine whether information should be classified as proprietary:

(a) The information reveals details of Framatome’s research and development plans and programs or their results.

(b) Use of the information by a competitor would permit the competitor to significantly reduce its expenditures, in time or resources, to design, produce, or market a similar product or service.

(c) The information includes test data or analytical techniques concerning a process, methodology, or component, the application of which results in a competitive advantage for Framatome.

(d) The information reveals certain distinguishing aspects of a process, methodology, or component, the exclusive use of which provides a competitive advantage for Framatome in product optimization or marketability.

(e) The information is vital to a competitive advantage held by Framatome, would be helpful to competitors to Framatome, and would likely cause substantial harm to the competitive position of Framatome.

The information in these Documents is considered proprietary for the reasons set forth in paragraphs 6(b), 6 (c), 6(d) and 6(e) above.

7. In accordance with Framatome's policies governing the protection and control of information, proprietary information contained in these Documents has been made available, on a limited basis, to others outside Framatome only as required and under suitable agreement providing for nondisclosure and limited use of the information.

8. Framatome policy requires that proprietary information be kept in a secured file or area and distributed on a need-to-know basis.

9. The foregoing statements are true and correct to the best of my knowledge, information, and belief.

I declare under penalty of perjury that the foregoing is true and correct.

Executed on November 19, 2020.

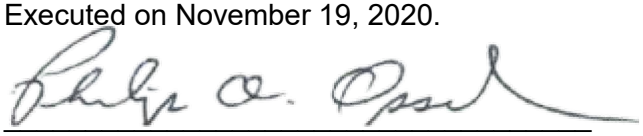

Philip A. Opsal

Attachment 5

"Peach Bottom 2 N16A Instrument Nozzle Repair J-Groove One-Cycle Justification Non-Proprietary," Document Number 32-9321037–001 (Non-Proprietary Version)

framatome

CALCULATION SUMMARY SHEET (CSS)

Document No. 32 - 9321037 - 001 Safety Related: ☒Yes ☐ No

Title Peach Bottom 2 N16A Instrument Nozzle Repair J-Groove One-Cycle Justification Non-Proprietary

PURPOSE AND SUMMARY OF RESULTS:

PURPOSE:

During the P2R23 outage, a leakage was discovered at the Reactor Pressure Vessel (RPV) Instrument Nozzle 16A at Peach Bottom Atomic Power Station Unit 2 (Peach Bottom Unit 2), which is a radial nozzle extending horizontally from the cylindrical vessel shell. Per Reference [20], an EVT-1 examination performed identified a crack extending vertically downward from the 6 o'clock position of the nozzle.

A half nozzle repair was designed in which portion of the existing nozzle will be severed and a replacement nozzle will be attached to the OD of the reactor pressure vessel (References [3] and [4]). The present concern is that the flaw in the remnant J-Groove weld could impact the structural integrity of the vessel. Since the hoop stress in the vessel at the J-groove weld is greater than the axial stress at the same location, the preferential direction for cracking is radial relative to the nozzle and axial relative to the vessel. Therefore, a radial-axial flaw is postulated to extend from the J-Groove weld bore through the entire J-Groove weld length up to the indication length in the RPV shell axis direction and up to the J-Groove weld depth in the original nozzle axis direction. The purpose of this analysis is to evaluate the postulated radial-axial flaw for one fuel cycle of operation.

The purpose of Revision 001 of this document is to incorporate editorial comments on the bracketing of Proprietary information.

SUMMARY OF RESULTS:

Based on a combination of Linear Elastic Fracture Mechanics (IWB-3610 of ASME Section XI, Reference [8]) and Elastic Plastic Fracture Mechanics (ASME Code Case N-749, Reference [9] , with applicable conditions per Table 2 of Reg. Guide 1.147, Revision 19, Reference [17]), the postulated flaw in the as-left J-groove weld of nozzle N16A at Peach Bottom Unit 2 is shown to be acceptable for one fuel cycle following the P2R23 outage. Results are summarized in Section 7.0.

Note: Proprietary information in this document is indicated by bolded brackets (**[ ]**).
The Proprietary version of this document is 32-9321034-002.

If the computer software used herein is not the latest version per the EASI list, AP 0402-01 requires that justification be provided.

THE FOLLOWING COMPUTER CODES HAVE BEEN USED IN THIS DOCUMENT:

CODE/VERSION/REV	CODE/VERSION/REV
ANSYS 19.2 (Section A.6)	

THE DOCUMENT CONTAINS ASSUMPTIONS THAT SHALL BE VERIFIED PRIOR TO USE

☐Yes
☒ No

Review Method: ☒ Design Review (Detailed Check)

☐ Alternate Calculation

Does this document establish design or technical requirements? ☐ YES ☒ NO

Does this document contain Customer Required Format? ☐ YES ☒ NO

Signature Block

Name and Title (printed or typed)	Signature	P/R/A/M and LP/LR	Date	Pages/Sections Prepared/Reviewed/Approved
Luziana Matte Technical Consultant	*LR MATTE* *11/19/2020*	LP		All Pages/ All Sections
Ashok Nana Advisory Engineer	*AD NANA* *11/19/2020*	LR		All Pages/ All Sections
David Cofflin Supervisory Engineer	*D KIM* *for DR COFFLIN* *11/19/2020*	A		All Pages/ All Sections

Notes: P/R/A designates Preparer (P), Reviewer (R), Approver (A);
LP/LR designates Lead Preparer (LP), Lead Reviewer (LR);
M designates Mentor (M)

In preparing, reviewing and approving revisions, the lead preparer/reviewer/approver shall use 'All' or 'All except ___' in the pages/sections reviewed/approved. 'All' or 'All except ___' means that the changes and the effect of the changes on the entire document have been prepared/reviewed/approved. It does not mean that the lead preparer/reviewer/approver has prepared/reviewed/approved all the pages of the document.

With Approver permission, calculations may be revised without using the latest CSS form. This deviation is permitted when expediency and/or cost are a factor. Approver shall add a comment in the right-most column that acknowledges and justifies this deviation.

Project Manager Approval of Customer References and/or Customer Formatting (N/A if not applicable)

Name (printed or typed)	Title (printed or typed)	Signature	Date	Comments
Alan Stalker	Project Manager	*AR STALKER* *11/19/2020*		

Record of Revision

Revision No.	Pages/Sections/Paragraphs Changed	Brief Description / Change Authorization
000	All	Original Release (November 2020). The Proprietary version of this document is 32-9321034-001.
001	All	Incorporate editorial comments on the bracketing of Proprietary information on Table A-1 and Figure A-1. The Proprietary version of this document is 32-9321034-002.

Table of Contents

Page

SIGNATURE BLOCK 2

RECORD OF REVISION 3

LIST OF TABLES 6

LIST OF FIGURES 7

1.0 PURPOSE 8

2.0 ANALYTICAL METHODOLOGY 12
- 2.1 Stress Intensity Factor Solution 12
- 2.2 Fatigue and Stress Corrosion Crack Growth 17
- 2.3 Linear Elastic Fracture Mechanics 17
- 2.4 Elastic Plastic Fracture Mechanics 18
  - 2.4.1 Screening Criteria 18
  - 2.4.2 Flaw Stability and Crack Driving Force 18
- 2.5 Acceptance Criteria 19
- 2.6 Primary Stress Evaluation 20

3.0 ASSUMPTIONS 21
- 3.1 Unverified Assumptions 21
- 3.2 Justified Assumptions 21
- 3.3 Modeling Simplifications 22

4.0 DESIGN INPUTS 23
- 4.1 Geometry 23
- 4.2 Materials 24
  - 4.2.1 Mechanical Properties 24
  - 4.2.2 Fracture Material Properties 25
- 4.3 Applied Stresses 26
  - 4.3.1 Operating Stresses 26
  - 4.3.2 Weld Residual Stress 26
  - 4.3.3 Crack Face Pressure 27

5.0 COMPUTER USAGE 27
- 5.1 Computer Software 27
- 5.2 Computer Files 27

6.0 CALCULATIONS 28
- 6.1 LEFM Evaluation 28
- 6.2 EPFM Evaluation 28
- 6.3 Primary Stress Evaluation 29

Table of Contents
(continued)

Page

7.0 CONCLUSIONS 30

8.0 REFERENCES 32

APPENDIX A : OPERATING STRESS ANALYSIS 34

APPENDIX B : SIF SOLUTION TEST CASES 50

APPENDIX C : FM EVALUATION RESULT TABLES 53

List of Tables

Page

Table 2-1: Structural Factors for Flaw Acceptance 20
Table 4-1: Key Dimensions 23
Table 4-2: Material Properties for Reactor Pressure Vessel 24
Table 4-3: Applicable Operating Transient 26
Table 5-1: Computer Files 27
Table A-1: Material Designations 35
Table A-2: Heat Up and Cool Down 37
Table A-3: Loss of [ ] Pump, [ ] 39
Table A-4: [ ] Overpressure [ ] 41
Table A-5: Single Relief [ ] 43
Table A-6: Column Description 47
Table A-7: List of Computer Files for Revision 000 49
Table C-1: LEFM Results – HUCD Transient 54
Table C-2: LEFM Results – Loss of [ ] Pump Transient 55
Table C-3: LEFM Results – [ ] Overpressure [ ] Transient 56
Table C-4: LEFM Results – Single Relief [ ] Transient 57
Table C-5: EPFM Results (Section 3.1 of CC N-749) – HUCD Transient 58
Table C-6: EPFM Results (Section 3.1 of CC N-749) – Loss of [ ] Pump Transient 59
Table C-7: EPFM Results (Section 3.1 of CC N-749) – [ ] Overpressure [ ] Transient 60
Table C-8: EPFM Results (Section 3.1 of CC N-749) – Single Relief [ ] Transient 61

List of Figures

Page

Figure 1-1: Instrumentation Nozzle N16-A - Vertical Crack Extending Down from 6 O'clock Position 9
Figure 1-2: Instrumentation Nozzle N16-A Repair Configuration with Temporary Nozzle Dam 10
Figure 1-3: Postulated Radial-Axial Flaw Configuration 11
Figure 2-1: SIF Solution Model 13
Figure A-1: Material Assignment 36
Figure A-2: Heat Up and Cool Down 38
Figure A-3: Loss of [ ] Pump, [ ] 40
Figure A-4: [ ] Overpressure [ ] 42
Figure A-5: Single Relief [ ] 44
Figure A-6: Locations for Thermal Gradients 45
Figure A-7: FE Model, Crevice Boundary Conditions 46
Figure A-8: Structural Run Boundary Conditions 46
Figure A-9: Results, Reported Locations 47
Figure B-1: Test Case for Tension (Based on Figure 10 of [5]) 51
Figure B-2: Test Case for Bending (Based on Figure 11 of [5]) 52

1.0 PURPOSE

During the P2R23 outage, a leakage was discovered at the Reactor Pressure Vessel (RPV) Instrument Nozzle 16A (40° azimuth) at Peach Bottom Atomic Power Station Unit 2 (Peach Bottom Unit 2), which is a radial nozzle extending horizontally from the cylindrical vessel shell (References [1] and [2]). Per Reference [20], an EVT-1 examination performed identified a crack extending vertically downward from the 6 o'clock position of the nozzle with an approximate length of **[ ]** from the ID of the original nozzle (Figure 1-1).

A half nozzle repair was designed in which portion of the existing nozzle will be severed and a replacement nozzle will be attached to the OD of the reactor pressure vessel (References [3] and [4]) (Figure 1-2). The present concern is that a flaw in the remnant J-Groove weld could impact the structural integrity of the vessel. Since the hoop stress in the vessel at the J-groove weld is greater than the axial stress at the same location, the preferential direction for cracking is radial relative to the nozzle and axial relative to the vessel. Therefore, since Reference [20] does not provide measurements on the indication depth, a radial-axial flaw is postulated (consistent with and to bound the actual observed indication) to extend from the J-Groove weld bore through the entire J-Groove weld up to the indication length in the RPV shell axis direction and up to the J-Groove weld depth in the original nozzle axis direction (Figure 1-3) (Modelling Simplification listed in Section 3.3 item 2). The purpose of this analysis is to evaluate the postulated radial-axial flaw for one fuel cycle of operation.

Purpose of Revision 001 of 32-9321034 is to indicate the Proprietary information in this document by bolded brackets (**[ ]**).

Purpose of Revision 002 of 32-9321034 is to incorporate editorial comments on the bracketing of Proprietary information.

Figure 1-1: Instrumentation Nozzle N16-A - Vertical Crack Extending Down from 6 O'clock Position

Figure 1-2: Instrumentation Nozzle N16-A Repair Configuration with Temporary Nozzle Dam

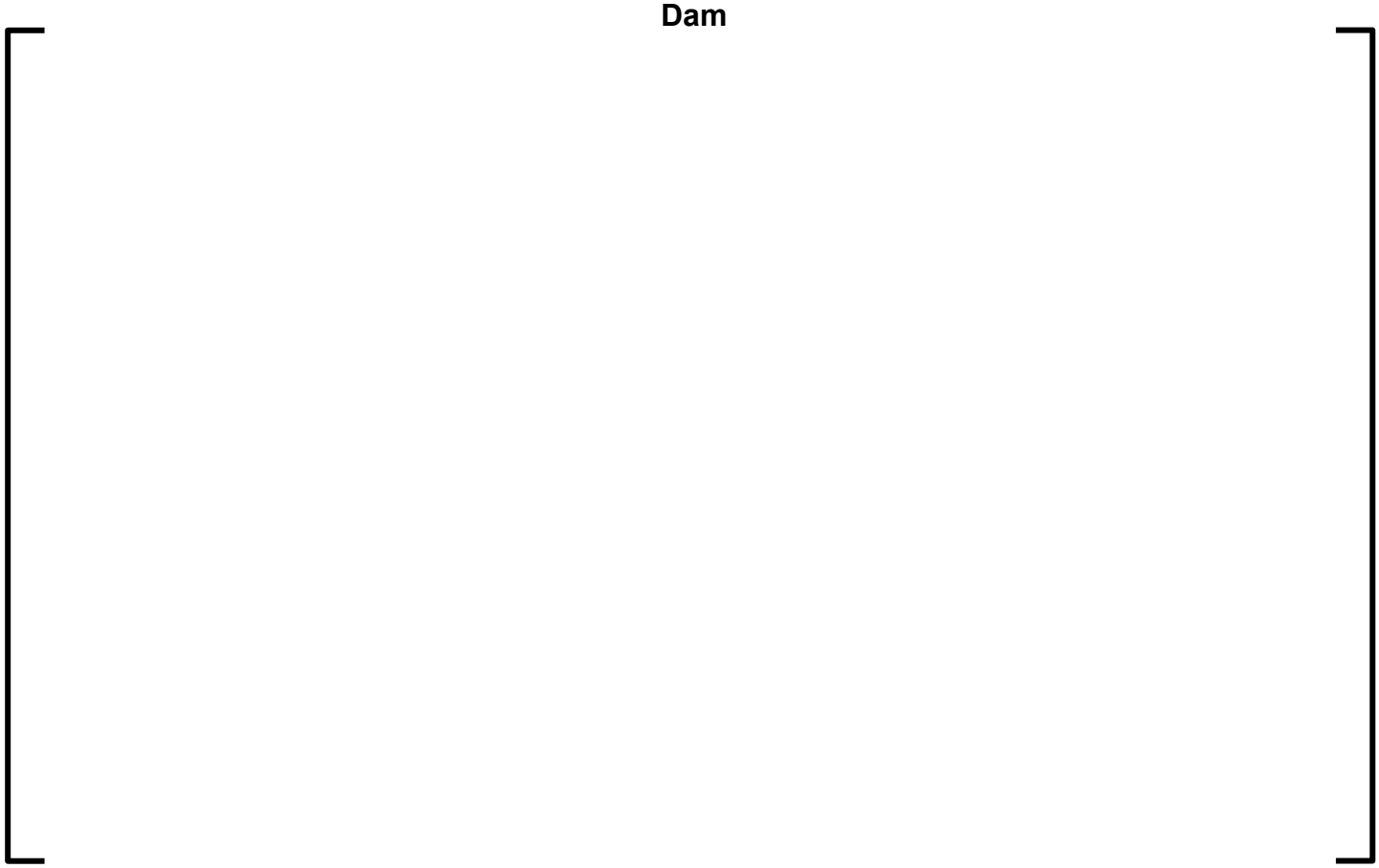

Figure 1-3: Postulated Radial-Axial Flaw Configuration

2.0 ANALYTICAL METHODOLOGY

A radial-axial flaw at the inside corner of the nozzle penetration is evaluated based on linear elastic fracture mechanics (LEFM) and elastic plastic fracture mechanics (EPFM), as outlined below.

1. Postulate an initial radial-axial flaw in the J-groove weld, extending from the J-Groove weld bore through the entire J-Groove weld up to the indication length in the RPV shell axis direction (initial flaw length c_0 in Figure 1-3) and up to the J-Groove weld depth in the original nozzle axis direction (initial flaw depth a_0 in Figure 1-3) (Modelling Simplification listed in Section 3.3 item 2).
2. Estimate the total flaw growth accommodating any potential crack growth into the RPV vessel wall, using [ ] Reference [13], as a basis for the crack growth rates (CGR).
3. Calculate the applied stress intensity factors for selected limiting transients using the stress intensity factor (SIF) solution from reference [5] for the estimated final flaw sizes at the end of one fuel cycle.
4. Compare the applied stress intensity factors to the ASME Section XI code criteria of IWB-3612 and IWB-3613 (Reference [8]) as applicable.
5. Calculate the applied J-integral with appropriate safety factors as defined in Section 3.1 of ASME Code Case N-749 (Reference [9]).
6. Compare the applied J-integral to the material J-integral at a ductile crack extension of *0.1 inch*, which will be based on the lower bound J-R curve in Reg. Guide 1.161 (Reference [15]).
7. If the criteria of Section 3.1 of Reference [9] are not met, the flaw may still be acceptable if the criteria of Section 3.2 of Reference [9] are met. In this case, the applied J-integral with appropriate safety factors as defined in Section 3.2 of ASME Code Case N-749 (Reference [9]) is also calculated.
8. If the criteria of Section 3.2 of ASME Code Case N-749 (Reference [9]) are required, a flaw stability analysis is also performed using a *J*-integral/tearing modulus (*J-T*) diagram to evaluate flaw stability under ductile tearing. The flaw stability is demonstrated at an applied *J*-integral when the applied tearing modulus is less than the material tearing modulus. Alternately, the applied *J*-integral is less than the J-integral at the point of instability.
9. Verify the primary stress, assuming a local area reduction of the pressure retaining membrane that is equal to the area of the flaw, meets the limits of NB-3200 rules, Reference [11], as required by IWB-3610(d)(2) (Reference [8]) and Sections 3.1(c) or 3.2(a)(3) of N-749 (Reference [9]).

Additional details on the methodology are provided in the following subsections.

2.1 Stress Intensity Factor Solution

The stress intensity factor (SIF) solution for a quarter-elliptical corner crack initiating at the bore of a cylindrical penetration from Reference [5], as shown in Figure 2-1, is used in the current flaw evaluation analysis to develop the applied stress intensity factor at the crack tip.

Figure 2-1: SIF Solution Model

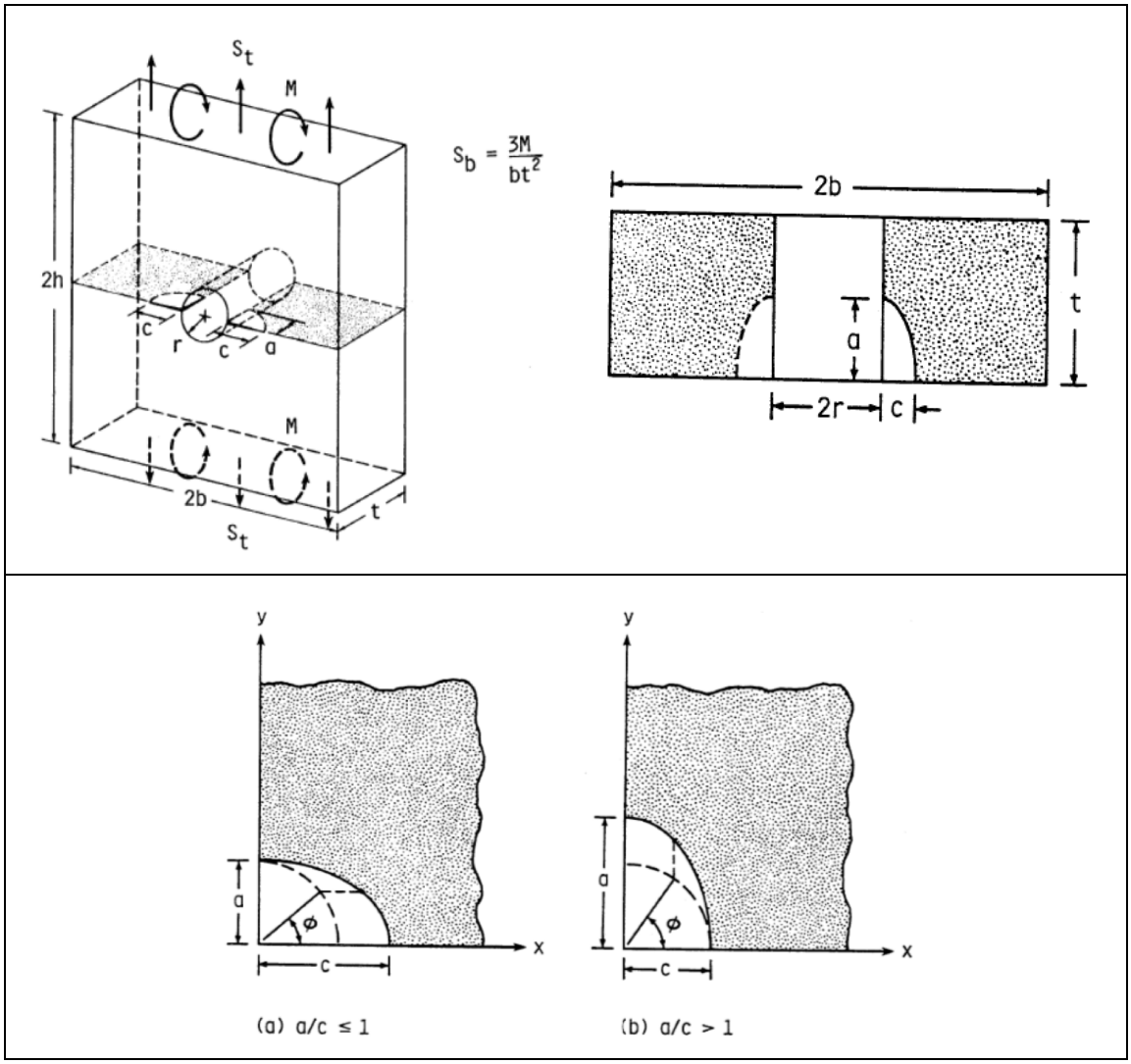

The formulas for the SIF solution as developed in Reference [5] are documented as follows:

$$K = (F_{ch}S_t + F_{chb}H_{ch}S_b)\sqrt{\frac{\pi a}{Q}}\sqrt{\frac{\frac{4}{\pi}+\frac{ac}{2tr}}{\frac{4}{\pi}+\frac{ac}{tr}}}$$

Where S_t is the membrane stress, S_b is the bending stress, a is the flaw size (nozzle axis) in the depth direction, c is the flaw size in the lateral (radial) direction, t is the plate thickness, and r is the hole radius. The final factor in the equation converts the solution for two symmetric flaws into an equation for one flaw. The remaining terms are defined below as reported in Reference [5]. The flaw evaluation in this document will be based on the depth location, which produce higher applied stress intensity values. The solution in Reference [5] was curve fitted for the range of parameters $0.2 < a/c < 2$, $a/t < 1$, $0.5 \le r/t \le 2$, $(r + c)/b < 0.5$, and $-\pi/2 \le \phi \le -\pi/2$. It should be noted that the r/t ratio for the geometry analyzed in the current flaw evaluation is < 0.5. However, the Reference [5] SIF solution still provides reasonable and conservative estimation of the crack driving force. The parameter b is the plate half width. It is used for finite width correction factor ('f_w' equation below), which is a factor that accounts for cases where the edge of the flaw at distance "$r+c$" from the hole centerline in Figure 2-1 reaches near the edge of the plate at distance "b" from the hole centerline. The factor approaches 1.0 as the plate width "b" becomes large. Since the RPV is very large and the crack is not near an edge of the RPV this factor is essentially 1.0. Hence, the solution is not sensitive to the parameter b. The solution is implemented in an Excel spreadsheet. Tests of the spreadsheet to verify the implementation of the equations are shown in Appendix B. The equations from Reference [5] are presented below:

$$F_{ch} = \left[M_1 + M_2\left(\frac{a}{t}\right)^2 + M_3\left(\frac{a}{t}\right)^4\right] \times g_1 \times g_2 \times g_3 \times g_4 \times f_\phi \times f_w$$

$$F_{chb} = \left[M_1 + M_2\left(\frac{a}{t}\right)^2 + M_3\left(\frac{a}{t}\right)^4\right] \times g_1 \times g_{2b} \times g_3 \times g_4 \times f_\phi \times f_w$$

$$H_{ch} = H_1 + (H_2 - H_1) \times (sin\phi)^p$$

$$H_1 = 1 + G_{11} \times \frac{a}{t} + G_{12} \times \left(\frac{a}{t}\right)^2 + G_{13} \times \left(\frac{a}{t}\right)^3$$

$$H_2 = 1 + G_{21} \times \frac{a}{t} + G_{22} \times \left(\frac{a}{t}\right)^2 + G_{23} \times \left(\frac{a}{t}\right)^3$$

$$f_\phi = \left[\left(\frac{a}{c}\right)^2 \times (cos\phi)^2 + (sin\phi)^2\right]^{0.25}$$

$f_w = \left\{sec\left(\frac{\pi r}{2b}\right) \times sec\left[\frac{\pi(2r+nc)}{4(b-c)+2nc} \times \sqrt{\frac{a}{t}}\right]\right\}^{0.5}$, where $n = 1$ is for a single crack and $n = 2$ is for two-symmetric cracks

The factor g_2 is different for tension and bending loads. For tension, g_2 is determined as below with $\mu=0.85$

$$g_2 = \frac{1 + 0.358\lambda + 1.425\lambda^2 - 1.578\lambda^3 + 2.156\lambda^4}{1 + 0.13\lambda^2}$$

$$\lambda = \frac{1}{1 + \frac{c}{r} \times cos(\mu\phi)}$$

For bending, g_{2b} is determined as below

$$g_{2b} = \frac{1 + 0.358\lambda_b + 1.425{\lambda_b}^2 - 1.578{\lambda_b}^3 + 2.156{\lambda_b}^4}{1 + 0.13{\lambda_b}^2}$$

$$\lambda_b = \frac{1}{1 + \frac{c}{r} \times cos(\mu_b \phi)}$$

$$\mu_b = 0.85 - 0.25\left(\frac{a}{t}\right)^{0.25}$$

For $a/c \leq 1$

$$M_1 = 1.13 - 0.09\left(\frac{a}{c}\right)$$

$$M_2 = -0.54 + \frac{0.89}{0.2 + \frac{a}{c}}$$

$$M_3 = 0.5 - \frac{1}{0.65 + \frac{a}{c}} + 14\left(1 - \frac{a}{c}\right)^{24}$$

$$g_1 = 1 + \left[0.1 + 0.35\left(\frac{a}{t}\right)^2\right] \times (1 - sin\phi)^2$$

$$g_3 = \left(1 + 0.04\frac{a}{c}\right) \times [1 + 0.1(1 - cos\phi)^2] \times \left[0.85 + 0.15\left(\frac{a}{t}\right)^{0.25}\right]$$

$$g_4 = 1 - 0.7\left(1 - \frac{a}{t}\right) \times \left(\frac{a}{c} - 0.2\right)\left(1 - \frac{a}{c}\right)$$

$$p = 0.1 + 1.3\frac{a}{t} + 1.1\frac{a}{c} - 0.7\frac{a}{c}\left(\frac{a}{t}\right)$$

$$G_{11} = -0.43 - 0.74\frac{a}{c} - 0.84\left(\frac{a}{c}\right)^2$$

$$G_{12} = 1.25 - 1.19\frac{a}{c} + 4.39\left(\frac{a}{c}\right)^2$$

$$G_{13} = -1.94 + 4.22\frac{a}{c} - 5.51\left(\frac{a}{c}\right)^2$$

$$G_{21} = -1.5 - 0.04\frac{a}{c} - 1.73\left(\frac{a}{c}\right)^2$$

$$G_{22} = 1.71 - 3.17\frac{a}{c} + 6.84\left(\frac{a}{c}\right)^2$$

$$G_{23} = -1.28 + 2.71\frac{a}{c} - 5.22\left(\frac{a}{c}\right)^2$$

$$Q = 1 + 1.464 \times \left(\frac{a}{c}\right)^{1.65}$$

For $a/c > 1$

$$M_1 = \sqrt{\frac{c}{a}}\left(1 + 0.04\frac{c}{a}\right)$$

$$M_2 = 0.2\left(\frac{c}{a}\right)^4$$

$$M_3 = -0.11\left(\frac{c}{a}\right)^4$$

$$g_1 = 1 + \left[0.1 + 0.35\frac{c}{a}\left(\frac{a}{t}\right)^2\right] \times (1 - sin\phi)^2$$

$$g_3 = \left(1.13 - 0.09\frac{c}{a}\right) \times [1 + 0.1(1 - cos\phi)^2] \times \left[0.85 + 0.15\left(\frac{a}{t}\right)^{0.25}\right]$$

$$g_4 = 1$$

$$G_{11} = -2.07 + 0.06\frac{c}{a}$$

$$G_{12} = 4.35 + 0.16\frac{c}{a}$$

$$G_{13} = -2.93 - 0.3\frac{c}{a}$$

$$G_{21} = -3.64 + 0.37\frac{c}{a}$$

$$G_{22} = 5.87 - 0.49\frac{c}{a}$$

$$G_{23} = -4.32 + 0.53\frac{c}{a}$$

$$Q = 1 + 1.464 \times \left(\frac{c}{a}\right)^{1.65}$$

$$p = 0.2 + \frac{c}{a} + 0.6\frac{a}{t}$$

After determining the SIF value from the equations listed above, a plasticity correction is applied based on the Irwin plastic zone correction. The Irwin plastic zone correction is discussed in Reference [6]. The effective crack depth is defined as the sum of the actual crack size and the plastic zone correction:

$$a_{eff} = a + r_y$$

Where r_y for plane strain conditions the correction is (Reference [6], Eq. 2.63):

$$r_y = \frac{1}{6\pi}\left(\frac{K_I}{\sigma_{ys}}\right)^2$$

Where σ_{ys} is the yield strength of the material and K_I is the stress intensity factor at the actual crack size (depth a and length c). The plastic zone correction is applied to the flaw length, c, using the applied K_I at the surface point (ϕ=0°), and to the flaw depth, a, using the applied K_I at the deepest point (ϕ=90°). An effective stress intensity factor (K_{Ieff}) is calculated by first calculating K_I based on flaw size a and c. Then the size of the plastic zone at a and c (r_y at ϕ=90° and ϕ=0°) is calculated based on K_I at ϕ=90° and ϕ=0°, respectively. Then the K_{Ieff} is determined by recalculating K_I utilizing the flaw dimension $a + r_y$ (ϕ=90°) and $c + r_y$ (ϕ=0°) in place of a and c, respectively.

2.2 Fatigue and Stress Corrosion Crack Growth

Flaw growth in the low alloy steel is driven by fatigue crack growth and intergranular stress corrosion cracking (IGSCC). Since the current analysis considers only one fuel cycle of plant operation, fatigue crack growth will be minimal.

The analysis conservatively postulates that a flaw extends through the entire J-groove weld. [

]

For one fuel cycle of operation [ ] the total [ ] growth is equal to [ ] The postulated flaw depth and length conservatively assumes a total flaw growth of [ ] which provides sufficient margin to accommodate any potential crack growth.

2.3 Linear Elastic Fracture Mechanics

Linear Elastic Fracture Mechanics (LEFM) acceptance criteria are based on the criteria of IWB-3600 of Reference [8]. Article IWB-3612 of Section XI requires that the applied stress intensity factor be less than the available fracture toughness at the crack tip temperature, with appropriate safety factor, as outlined below.

IWB-3613(a): For conditions where pressurization does not exceed 20% of the design pressure (design pressure is [ ] Reference [2]) during which the minimum temperature is not less than RT_{NDT}:

$K_I < K_{Ic} / \sqrt{2}$

IWB-3613(b): For Normal and Upset conditions excluding those described in IWB-3613(a):

$K_I < K_{Ic} / \sqrt{10}$ (criteria of IWB-3612(a))

IWB-3613(c): For Emergency and Faulted conditions:

$K_I < K_{Ic} / \sqrt{2}$ (criteria of IWB-3612(b))

In the above, K_{Ic} is the fracture toughness based on crack initiation defined in A-4200(b) of Reference [8].

2.4 Elastic Plastic Fracture Mechanics

The Elastic Plastic Fracture Mechanics (EPFM) analysis uses ASME Code Case N-749 (Reference [9]). The methodology is described in the following subsections.

2.4.1 Screening Criteria

ASME Code Case N-749 states that EPFM acceptance criteria are applicable to ferritic steel components on the upper shelf of the Charpy energy curve when the metal temperature exceeds the upper shelf transition temperature, T_c. The NRC has proposed a modification to the Code Case definition of T_c (Reference [10]), which is considered for this analysis and defined below

$$T_c = 154.8°\text{F} + 0.82 \times RT_{NDT} \quad \text{(U.S. Customary Units)}$$

Where RT_{NDT} is the adjusted reference nil-ductility temperature as described in Section 4.2.2. When the metal temperature exceeds T_c, EPFM analysis is applicable. Additionally, NRC defines in RG 1.147 draft rev. 19 (Reference [17]), a temperature T_{c1} below which the LEFM method must be applied:

$$T_{c1} = 95.36°\text{F} + 0.703 \times RT_{NDT} \quad \text{(U.S. Customary Units)}$$

Per Reference [17], between T_{c1} and T_c, while the fracture mode is in transition from LEFM to EPFM, users should consider whether or not it is appropriate to apply the EPFM method.

2.4.2 Flaw Stability and Crack Driving Force

Elastic-plastic fracture mechanics analysis will be performed based on ASME Code Case N-749 (Reference [9]) to evaluate crack driving force and flaw stability (if applicable). Two possible sets of acceptance criteria for EPFM are defined in Code Case N-749:

- Section 3.1 Acceptance Criteria Based Solely on Limited Ductile Crack Extension, or
- Section 3.2 Acceptance Criteria Based on Limited Ductile Crack Extension and Stability.

Section 3.1 of Reference [9] states that the flaw is acceptable if the crack driving force, as measured by the applied J-integral (J_{app}) with appropriate structural factors applied to the loads, is less than the *J*-integral of the material (J_{mat}) at a ductile crack extension of *0.1 inch* ($J_{0.1}$). If the criteria of Section 3.1 of Reference [9] are not met, the flaw may still be acceptable if the criteria of Section 3.2 of Reference [9] are met. Section 3.2 allows lower safety factors for the crack driving force check, and additionally requires that flaw stability be evaluated with appropriate safety factors.

If applicable, the flaw stability analysis is performed using a *J*-integral/tearing modulus (*J*-*T*) diagram to evaluate flaw stability under ductile tearing, where *J* is either the applied (J_{app}) or the material (J_{mat}) *J*-integral, and *T* is the tearing modulus, defined as $(E/\sigma_f^2)\times(\partial J/\partial a)$. Flaw stability and crack driving force assessments utilizes the safety factors from Code Case N-749 as outlined in Table 2-1.

The general methodology for performing an EPFM analyses is outlined below.

$E' = E/(1-\nu^2)$
K_I due to pressure (primary) = K_{Ip}
K_I due to thermal loads (secondary) = K_{Is}
Safety factor on primary loads = SF_p
Safety factor on secondary loads = SF_s
Total applied K_I with safety factors, $K_{Ieff} = SF_p \times K_{Ip} + SF_s \times K_{Is}$

Where E and ν are the modulus of elasticity and Poisson's ratio, as specified in Section 4.2.1.

For this analysis the crack driving force, J, is estimated based on small scale yielding as described below. The stress intensity factors due to primary stresses (K_{Ip}) and the stress intensity factors due to secondary stresses (K_{Is}) are calculated using the method described in Section 2.1, including the plastic zone correction, which is applied prior to application of structural factors per Section 4.1 of Reference [9]. Per Sections 2(c) of Reference [9], residual stresses do not need to be included in the EPFM analysis.

The applied J-integral is then calculated using the following relationship:

$$J_{app} = \frac{(K_{Ieff})^2}{E'}$$

The applied J-integral is checked against $J_{0.1}$, demonstrating that the crack driving force falls below the J-R curve at a crack extension of 0.1 inch, per Section 3.1 of Reference [9].

If applicable, for flaw stability analysis (i.e., Section 3.2 of Reference [9]), the final parameter needed to construct the J-T diagram is the tearing modulus. The applied tearing modulus, T_{app}, is calculated by numerical differentiation for small increments of crack size (da) about the crack size (a), according to

$$T_{app} = \frac{E}{\sigma_f^2}\left(\frac{J_{app}(a+da) - J_{app}(a-da)}{2\,da}\right)$$

Where σ_f is the flow stress defined as $\sigma_f = ½(\sigma_y + \sigma_u)$, where σ_y is the yield strength and σ_u is the ultimate tensile strength, as specified in Section 4.2.1.

The J-integral resistance (J-R) curve, needed for the EPFM method of analysis, is described in Section 4.2.2. The flaw stability is demonstrated at an applied J-integral when the applied tearing modulus is less than the material tearing modulus. Alternately, the applied J-integral is less than the J-integral at the point of instability.

2.5 Acceptance Criteria

The applicable code is ASME Section XI, 2013 Edition (Reference [8]). If the service life of the component is shown to be limited, an alternate approach of using ASME Section XI Code Case N-749 (Reference [9]) as modified by the Nuclear Regulatory Commission (Reference [10]) will be considered in the evaluation. Acceptance of each postulated flaw is determined based on available fracture toughness or ductile tearing resistance using the safety factors outlined in Table 2-1.

Table 2-1: Structural Factors for Flaw Acceptance

LEFM[1]			
Operating Condition	**Evaluation Method**	**Fracture Toughness / K_I**	
Normal/Upset	K_{IC} fracture toughness	$\sqrt{10} = 3.16$ or $\sqrt{2} = 1.41$[1a, 1b]	
Emergency/Faulted	K_{IC} fracture toughness	$\sqrt{2} = 1.41$[1c]	
EPFM Based on Limited Ductile Flaw Extension[2]			
Operating Condition	**Evaluation Method**	**Primary**	**Secondary**
Normal/Upset	$J_{0.1}$ limited flaw extension	2.0	1.0
Emergency/Faulted	$J_{0.1}$ limited flaw extension	1.5	1.0
EPFM Based on Limited Ductile Flaw Extension and Stability[3]			
Operating Condition	**Evaluation Method**	**Primary**	**Secondary**
Normal/Upset	J/T based flaw stability	2.14	1.0
Normal/Upset	$J_{0.1}$ limited flaw extension	1.5	1.0
Emergency/Faulted	J/T based flaw stability	1.2	1.0
Emergency/Faulted	$J_{0.1}$ limited flaw extension	1.25	1.0

Notes:

(1) LEFM safety factors are from IWB-3613 of ASME Section XI (Reference [8]).
   a. Per IWB-3613(a), for conditions where pressurization does not exceed 20% of the design pressure during which the minimum temperature is not less than RT_{NDT}:
      $K_I < K_{Ic} / \sqrt{2}$
   b. Per IWB-3613(b), for Normal and Upset conditions excluding those described in IWB-3613(a):
      $K_I < K_{Ic} / \sqrt{10}$ (criteria of IWB-3612(a))
   c. Per IWB-3613(c), for Emergency and Faulted conditions:
      $K_I < K_{Ic} / \sqrt{2}$ (criteria of IWB-3612(b))

(2) EPFM safety factors based on Section 3.1 of Code Case N-749 (Reference [9]).

(3) EPFM safety factors based on Section 3.2 of Code Case N-749 (Reference [9]).

2.6 Primary Stress Evaluation

IWB-3610(d)(2) of Reference [8] and Items 3.1(c) and 3.2(a)(3) of Reference [9] state that the flawed component must meet the primary stress limits of NB-3200, Reference [11], assuming a local area reduction of the pressure retaining membrane that is equal to the area of the flaw. For this evaluation, this check will be performed by confirming that the area of the flaw and any existing material removed by the modification are balanced by metal added by the weld pad, new J-groove weld, and fillet. Appropriate adjustments for difference in strengths of materials are made per the rules of NB-3336 (Reference [11]).

3.0 ASSUMPTIONS

3.1 Unverified Assumptions

There are no unverified assumptions used in this calculation.

3.2 Justified Assumptions

The following justified assumptions are used in this analysis:

1. Based on review of the stress-strain curves for [ ] in Reference [12], there is assumed to be a uniform weld residual stress of [ ] (slightly above room temperature yield) over the depth of the J-groove weld, which is balanced by a uniform compressive stress over the remaining thickness. This assumed stress distribution is then converted to an equivalent bending stress for use in the SIF solution described in Section 2.1. The equivalent bending stress S_b (estimated based on a local stress distribution) is applied as a remote stress, and would then be amplified by stress concentration effects accounted for in the SIF solution.

   This analysis simplifies the weld residual stress by constant stress with magnitude of [ ] over the whole cross section of the weld. Such simplification, although considered reasonable, is impossible to prove or disprove without detailed weld residual stress analysis which is far beyond the scope and time frame allowed by this OCJ.

[

]

Additional justified assumptions and modelling simplifications are listed in Section A.3 of Appendix A.

3.3 Modeling Simplifications

The following modeling simplifications are used in this analysis:

1. The SIF solution used (Section 2.1) is based on a corner flaw in a flat plate with a hole under remote uniaxial tension and bending stresses. This is a conservative simplification since the stress concentration at a hole is higher with uniaxial tension than with biaxial tension. The ratio of the hole radius to plate thickness, r/t is < 0.5, however the SIF solution of Reference [5] still provides a reasonable and conservative estimation of the crack driving force.
2. Two options were investigated to determine the more appropriate initial flaw length, c_o, and the bore radius, r, of the postulated flaw. The first option would be to utilize the initial flaw length as the indication length of [ ] and the bore radius as the original nozzle internal radius of [ ] (Table 4-1). The second option utilizes the initial flaw length as the indication length minus the original nozzle thickness [ ] (Table 4-1) and the bore radius as the J-Groove bore radius of [ ] The second option yields higher stress intensity factor values and is considered appropriate for use in this evaluation.

4.0 DESIGN INPUTS

4.1 Geometry

The original geometry is described in References [1] and [3], with the half nozzle repair design shown in Reference [3]. The reactor pressure vessel and the instrumentation nozzle 16A are described by the following key dimensions:

Table 4-1: Key Dimensions

Dimension	Value	Reference
Radius to Base Metal	[ ]	[3]
Reactor Vessel Wall Thickness (min)	[ ]	[3]
Cladding thickness	[ ]	[1] (note 2)
Inside Diameter of Original Nozzle	[ ]	[3]
Outside Diameter of Original Nozzle	[ ]	[3]
Depth of J-groove Weld (from cladding)	[ ]	[1] (note 2)
Width of J-Groove Weld	[ ]	[1] (note 2)
Diameter of Bore at J-Groove Weld	[ ]	[3]
Original Nozzle Thickness	[ ]	[3]

Note(s):

(1): Width of the J-groove weld is calculated as:

[ ]

(2): Drawing No. [ ], listed in Reference [1].

(3): [ ]

Per Reference [20], the vertical indication length is approximately [ ] from the ID of the original nozzle. Therefore, at the end of one fuel cycle, the postulated flaw length is taken as the indication length of [ ] (Reference [20]), minus the original nozzle thickness, plus the estimated total crack growth of [ ] (see Section 2.2).

The postulated flaw depth at the end of one fuel cycle is taken as the total depth of the J-groove weld, plus the estimated total crack growth of [ ] (see Section 2.2). This results in a flaw depth, a = [ ] and flaw length, c = [ ]

The thickness and the J-groove bore radius considered for the SIF solution is [ ] and [ ] respectively.

4.2 Materials

The materials used in the design are summarized below:

RV Shell	SA-302 Gr. B modified [ ]	Reference [4]
Existing J-Groove Weld	[ ]	Reference [3]
Existing Nozzle	[ ]	Reference [4]
Replacement Nozzle	[ ] UNS N06690 (Alloy 690)	Reference [4]
Repair Weld and Nozzle to Weld Pad Weld	ERNiCrFe-7A, UNS N066054, (Alloy 52M)	Reference [4]

4.2.1 Mechanical Properties

The reactor pressure vessel shell analyzed is made of SA-302 Grade B modified [ ] Reference [4]. Table 4-2 lists the temperature dependent values of modulus of elasticity (E), Poisson's ratio (ν), yield strength (σ_y), and ultimate strength (σ_u). These properties are obtained from References [14] and Reference [26] for the existing materials and Reference [23] for the modification materials, except for Poisson's ratio, where *0.3* is a typical value used in structural analysis.

Table 4-2: Material Properties for Reactor Pressure Vessel

Component	Reactor Pressure Vessel				
Material	SA-302 Grade B modified				
Temperature [°F]	$E^{(1)}$ [10^6 psi]		$\sigma_y{}^{(1)}$ [ksi]	[ ]	$\sigma_u{}^{(1)}$ [ksi]
70	29.9	0.30	50.0	[ ]	80.0
100	29.8	0.30	50.0	[ ]	---
200	29.5	0.30	47.2	[ ]	---
300	29.0	0.30	45.3	[ ]	---
400	28.6	0.30	44.5	[ ]	---
500	28.0	0.30	43.2	[ ]	---
600	27.4	0.30	42.0	[ ]	---

Notes:

(1): Per Reference [14].

(2): [

]

[ ] Per References [14] and [23], at a representative temperature of *550°F*, the design stress intensity, *Sm,* for [ ] and Alloy 690 is [ ] and the *Sm* for the SA-302 Grade B modified base metal is [ ]

4.2.2 Fracture Material Properties

Per Reference [19], the *54* EFPY adjusted reference nil-ductility temperature RT_{NDT} (ART) of the limiting material for the lower intermediate RV shell [ ] is [ ] and is conservatively considered for this analysis although the EFPY at the end of one-fuel cycle following the P2R23 outage is much lower (EFPY at the end of the P2R23 outage is [ ] per Reference [18]) (Justified Assumption listed in Section 3.2, item 5). This value of RT_{NDT} is utilized with the K_{Ic} fracture toughness for crack initiation curve defined in Article A-4200 of Section XI (Reference [8]) as:

$$K_{Ic} = 33.2 + 20.734 \exp[0.02(T - RT_{NDT})]$$

Where T is the crack tip temperature, K_{Ic} is in units of $ksi\sqrt{in}$, and T and RT_{NDT} are in units of °F. In the present calculations, K_{Ic} is limited to a maximum value of $200\ ksi\sqrt{in}$ (upper-shelf fracture toughness). The crack initiation K_{Ic} upper shelf toughness of $200\ ksi\sqrt{in}$ is achieved at $T\text{-}RT_{NDT}$ > [ ]

The *J*-integral resistance (*J*-*R*) curve, needed for the EPFM method of analysis, is obtained from the following correlation for reactor pressure vessel plate in Regulatory Guide 1.161, Section 3.3.1 (Reference [15]):

$$J_{mat} = MF\{C_1(\Delta a)^{C_2}\, exp(C_3(\Delta a)^{C_4})\}$$

Where *MF* is a margin factor, and Δa is the crack extension. C_1, C_2, C_3, and C_4 are coefficients which depend on the crack tip temperature and the Charpy V-notch upper-shelf energy as defined below:

$$C_1 = exp(-2.44 + 1.13\, ln(CVN) - 0.00277T)$$

$$C_2 = 0.077 + 0.116\, ln\, C_1$$

$$C_3 = -0.0812 - 0.0092\, ln\, C_1$$

$$C_4 = -0.409$$

Where *CVN* is the Charpy V-notch upper-shelf energy in ft-lbs, and T is the crack tip temperature in °F. The margin factor, *MF*, of *0.749* is utilized for the analysis for all cases, which provides a conservative *J*-*R* curve as required by Reference [9]. Section 3.3.1 of Reference [15] states that the use of this model should be justified if the sulfur content of the plate is greater than *0.018 wt.%*. Per Reference [2], the nozzle 16A is located in a section of shell course 2 with plate heat number [ ] Per Reference [18], plate [ ] has a sulfur content of [ ] and, therefore, the use of this model is applicable.

The actual Charpy V-notch upper shelf energy values in the longitudinal and transverse directions after one fuel cycle following the P2R23 outage (EFPY at the end of the P2R23 outage is [ ], Reference [18]) are not available. However, Reference [1] state that an equivalent margin analysis (EMA) was performed at *53* EFPY and approved by the NRC which confirms that the Charpy V-notch upper-shelf energy (*CVN*) is greater than [ ] Therefore, a *CVN* of [ ] is conservatively assumed in both the longitudinal and transverse directions for the one-cycle justification (Justified Assumption Section 3.2, item 2).

4.3 Applied Stresses

4.3.1 Operating Stresses

An axisymmetric finite element model is developed to generate transient stress results and is documented in Appendix A. The transients defined in Reference [1] are reviewed and the bounding transients are selected based on pressure and temperature ranges. Transient stress analyses are performed for the bounding design transients listed in Table 4-3, which are described in more detail in Appendix A:

Table 4-3: Applicable Operating Transient

Transient Name	Condition	ID
[ ]	Normal/Upset	HUCD
[ ]	Normal/Upset	Loss of Pump
[ ]	Emergency/Faulted	Overpressure
[ ]	Normal/Upset	Single Relief

Note (1): Applicable transients and conditions are defined in Reference [21].

The linearized through wall bending hoop stresses are taken from the finite element output for the path line '*NearPath*' through the RV shell, and contribute to the remote applied bending stress, S_b, used for the SIF solution. Since the finite element model uses an equivalent sphere with a radius of *2.5* times the actual radius, the membrane stresses are overly conservative, and thus the remote tensile stress, S_t, applied for the SIF solution is calculated using the basic hoop stress formula, pRi/t, where p is the pressure, Ri is the inside radius [ ] and t is the thickness [ ]

4.3.2 Weld Residual Stress

As noted in Section 3.2, item 1 it is assumed that the weld residual stress over the depth of the J-groove weld into the base metal, d = [ ] (Section 4.1) is at a uniform tensile stress of [ ] which is balanced by a uniform stress over the remainder of the total thickness [ ] such that the compressive stress is given by

[ ]

This stress distribution has a net tensile stress, S_t, of 0 ksi. The equivalent remote bending stress, S_b, is defined by

[ ]

4.3.3 Crack Face Pressure

Crack face pressure loading is accounted for in a similar manner to the welding residual stress. A uniform tensile stress equal to the applied pressure is considered over the crack depth, [ ] (Section 4.1). The stress over the remaining thickness is equal to zero. The equivalent remote tensile load is given by

[ ]

The equivalent bending stress for the postulated flaw depth is defined by

[ ]

5.0 COMPUTER USAGE

5.1 Computer Software

The calculations in the main body of this report are performed using Microsoft Excel spreadsheets. Documentation of the ANSYS (Reference [16]) runs reported in Appendix A are provided in that appendix.

5.2 Computer Files

The excel spreadsheet utilized for the fracture mechanics analysis is listed in Table 5-1 stored in ColdStor at the location listed below.

'\cold\General-Access\32\32-9000000\32-9321034-000\official'

Table 5-1: Computer Files

CRC Checksum	Size (Bytes)	Modified Date			Time	File Name
01269	418417	Nov	14	2020	11:09:47	*PeachBottom2_N16A_LEFM_EPFM_v1.xlsm*

6.0 CALCULATIONS

6.1 LEFM Evaluation

Applied stress intensity factors are calculated using the SIF solution from Section 2.1 and the various sources of stresses described in Section 4.3. The SIFs including plastic zone correction were calculated using the spreadsheet "*PeachBottom2_N16A_LEFM_EPFM_v1.xlsm*" (see Table 5-1) at both the ϕ=0° and ϕ=90° locations and compared to the acceptance criteria described in Sections 2.3 and 2.5. The K_{Ic} values shown in Table C-1 through Table C-4 are calculated using a temperature equal to the minimum of the metal temperature and the fluid temperature. For normal and upset conditions below a pressure of [ ] the criteria of IWB-3613(a) is considered such that the required margin is $\sqrt{2}$.

The upper shelf transition temperature, T_c defined in Section 2.4.1, above which the EPFM must be applied is calculated as follows:

$$T_c = 154.8°\text{F} + 0.82 \times RT_{NDT} = 154.8°\text{F} + 0.82 \times [\quad]$$

The additional temperature limit defined in RG 1.147 draft rev. 19 (Reference [17]), T_{c1} below which the LEFM method must be applied is calculated as follows

$$T_{c1} = 95.36°\text{F} + 0.703 \times RT_{NDT} = 95.36°\text{F} + 0.703 \times [\quad]$$

The results documented in Table C-1 through Table C-4 show that the Emergency and Faulted conditions transient satisfies the required LEFM margins in all cases. For the Normal and Upset conditions the low temperature/pressure cases satisfy the required LEFM margin. All cases which do not satisfy LEFM criteria are above the upper shelf transition temperature, T_c. Therefore, the EPFM method of analysis is applicable, and the results of that analysis are documented in Section 6.2.

Table C-1 through Table C-4 also show that LEFM requirements are met for all cases where the temperature conditions fall between T_{c1} and T_c, in which the fracture mode is in transition from LEFM to EPFM. Additionally, these cases are also evaluated for the EPFM method of analysis in Section 6.2.

6.2 EPFM Evaluation

The EPFM analysis is performed in the spreadsheet "*PeachBottom2_N16A_LEFM_EPFM_v1.xlsm*" (see Table 5-1) using the methodology described in Section 2.4. The same stresses used in Section 6.1 are used for the EPFM analysis, however, residual stresses are removed per Section 2(c) of code case N-749, Reference [9].

As noted in Section 4.3.1, the finite element model bending stresses are considered as secondary for the EPFM analysis. Although the Emergency and Faulted conditions satisfy the LEFM criteria, the EPFM evaluation is also performed for cases in the temperature range where EPFM ($T > T_c$) is applicable and for cases in the temperature range where fracture mode is in transition from LEFM to EPFM ($T_{c1} \leq T \leq T_c$).

Table C-5 through Table C-8 provide the results of the EPFM evaluations for the postulated flaw size using Section 3.1 of Code Case N-749 (Reference [9]). Results are shown with $J_{0.1}$ values using the assumed *CVN* of [ ] in both the longitudinal and transverse directions. The results are shown to be acceptable to the criteria of Section 3.1 of Code Case N-749 for all cases.

6.3 Primary Stress Evaluation

Primary stresses are evaluated as described in Section 2.6, by showing that the repair configuration adds sufficient amount of cross-sectional area to account for the reduction in cross-sectional area equal to the area of the postulated flaw. All areas calculated in the following lines are for one side of the symmetric configuration.

The area of the postulated J-groove flaw including the crack growth is calculated as the area of the trapezoid, with height equal to the flaw depth, *a*, base equal to the flaw length, *c*, and the weld prep angle of [ ] (Reference [1]).

Flaw Depth with crack growth, a =	[ ]	in
Flaw Length with crack growth, c =	[ ]	in
J-Groove Angle =	[ ]	°
Postulated Flaw Area, $A1$ = [ ] =	[ ]	in^2

The repair configuration adds material by the new Alloy 52M weld pad, J-groove weld, and fillet. The repair also exposes the low alloy steel to the reactor coolant, and per Reference [7] a corrosion rate of [ ] is applicable. For the calculation, the area removed from the low alloy steel will be increased by the ratio of *Sm* for SA-302 Gr. B to Alloy 690 and [ ] in order to account for the difference in strength per NB-3336 (Reference [11]).

Based on Reference [3], the area of Alloy 52M weld added by the repair pad, J-groove weld, and fillet is calculated as

Pad Diameter (Min), $D1$ =	[ ]	in
Nozzle Contigency Oversize Bore Diameter (Max), $D2$ =	[ ]	in
Pad Diameter (Max), $D3$ =	[ ]	in
Pad Thickness (Min), $t1$ =	[ ]	in
J-Groove Fillet Size, $t2$ =	[ ]	in
Pad + Fillet Area, $A2 = (D1-D2)/2 \times t1 + 0.5 \times t2^2 + (D3-D1)/2 \times t1/2$ =	[ ]	in^2

The low alloy steel area lost due the replacement nozzle bore and 20 years (conservatively used in lieu of the 2 years considered in the calculation) of corrosion is calculated as follows:

Max Contigency Oversize Bore Diameter, $D2$ =	[ ]	in
Original Bore Diameter, $D4$ =	[ ]	in
Conservative Max Bore Depth, $L1$ =	[ ]	in
Bore Area Removed, $A3 = (D2-D4)/2 \times L1$ =	[ ]	in^2
Conservative Exposed LAS Length, $L2$ =	[ ]	in
Radial Corrosion Loss, $R1$ = [ ] × *20 years*	[ ]	in
Corrosion Area Removed, $A4 = L2 \times R1$ =	[ ]	in^2
Total LAS Area Removed, $(A3+A4)$ =	[ ]	in^2
Sm(SA-302)/Sm(Alloy 690) =	[ ]	
Effective LAS Area Removed, $A5$ = [ ] × $(A3+A4)$ =	[ ]	in^2

The net area of the repair is calculated as follows:

Effective Area of the Repair, $A6 = (A2 - A5 - A1)$ =	[ ]	in^2

Since the net area added by the repair exceeds the area of the postulated flaw (*A6* = [ ] > *A1* = [ ]), the primary stress criteria of IWB-3610(d)(2) of Reference [8] and Sections 3.1(c) or 3.2(a)(3) of Reference [9] are considered to be satisfied for one fuel cycle.

7.0 CONCLUSIONS

Based on a combination of Linear Elastic Fracture Mechanics (IWB-3610 of ASME Section XI, Reference [8]) and Elastic Plastic Fracture Mechanics (ASME Code Case N-749, Reference [9], with applicable conditions per Table 2 of Reg. Guide 1.147, Revision 19, Reference [17]) evaluations, the postulated flaw in the as-left J-groove weld of nozzle 16A at Peach Bottom Unit 2 is shown to be acceptable for one fuel cycle following the P2R23 outage.

For temperatures below the upper shelf temperature, T_c, the LEFM analysis based on IWB-3610 (Reference [8]) criteria is applicable and the limiting cases are summarized below from Table C-1 through Table C-4:

Transient	**HUCD**	**Single Relief [ ]**
Service Level	Normal/Upset	Normal/Upset
Pressure (psig)	[ ]	[ ]
Temperature (°F)	[ ]	[ ]
K_{Ieff} (ksi√in)	[ ]	[ ]
K_{Ic} (ksi√in)	[ ]	[ ]
Margin, K_{Ic}/K_{Ieff}	[ ]	[ ]
Required Margin	[ ]	[ ]
Acceptable By LEFM?	Yes	Yes

For temperatures above the upper shelf temperature, T_c, and for temperatures between T_{c1} and T_c, in which the fracture mode is in transition from LEFM to EPFM per RG 1.147, Reference [17], the EPFM analysis based on Section 3.1 or 3.2 of the Code Case N-749 (Reference [9]) criteria is applicable and the limiting cases are summarized below from Table C-5 through Table C-8:

Transient	**Loss of [ ] Pumps**	**[ ] Overpressure [ ]**
Service Level	Normal/Upset	Emergency/Faulted
Pressure (psig)	[ ]	[ ]
Temperature (°F)	[ ]	[ ]
CVN USE (ft-lbs)	[ ]	[ ]
Applied J-Integral Check		
J_{app} (kips/in)	[ ]	[ ]
$J_{0.1}$ (kips/in)	[ ]	[ ]
Margin, $J_{app}/J_{0.1}$	[ ]	[ ]
Required Margin	[ ]	[ ]
Applied *J*-Integral Check Acceptable?	Yes	Yes
Stability Check Required?	No	No

The primary stress criteria of IWB-3610(d)(2) of Reference [8] and Section 3.1(c) or 3.2(a)(3) of Reference [9] are satisfied for one fuel cycle since the net area added by the repair exceeds the area of the postulated flaw as demonstrated in Section 6.3.

8.0 REFERENCES

References identified with an (*) are maintained within Exelon Records System and are not retrievable from Framatome Records Management. These are acceptable references per Framatome Administrative Procedure 0402-01, Attachment 7. See page 3 for Project Manager Approval of customer references.

1. [ ]
2. [ ]
3. [ ]
4. [ ]
5. Newman, JC and Raju, IS, "Stress-Intensity Factor Equations for Cracks in Three-Dimensional Finite Bodies Subjected to Tension and Bending Loads," NASA Technical Memorandum 85793.
6. T.L. Anderson, Fracture Mechanics: Fundamentals and Applications, CRC Press, 1991.
7. [ ]
8. ASME Boiler and Pressure Vessel Code, Section XI, "Rules for Inservice Inspection of Nuclear Power Plant Components", Division 1, 2013 Edition.
9. Cases of the ASME Boiler and Pressure Vessel Code, Case N-749, "Alternative Acceptance Criteria for Flaws in Ferritic Steel Components Operating in the Upper Shelf Temperature Range," Section XI, Division I.
10. Federal Register, Volume 81, Page 10787 (81 FR 10787), Wednesday March 2, 2016, Proposed Rules.
11. ASME Boiler and Pressure Vessel Code, Section III, "Rules for Construction of Nuclear Facility Components", Division 1, 2013 Edition.
12. [ ]
13. * [ ]
14. ASME Boiler and Pressure Vessel Code, Section III, Rules for Construction of Nuclear Vessels, 1965 Edition with 1965 Winter Addenda.
15. US NRC Regulatory Guide 1.161, "Evaluation of Reactor Pressure Vessels with Charpy Upper-Shelf Energy Less than 50 ft-lb", June 1995.
16. ANSYS Finite Element Computer Code, Version 19.2, ANSYS Inc., Canonsburg, PA.
17. DRAFT Regulatory Guide DG-1342, Inservice Inspection Code Case Acceptability, ASME Section XI, Division 1, Proposed Revision 19 of Regulatory Guide 1.147, dated August 2018 (ADAMS No. ML18114A225).

18. [ ]
19. Peach Bottom Atomic Power Station Units 2 and 3, Revision 26 to Updated Final Safety Analysis Report, Section 4.0, Reactor Coolant System, Part 1 of 2, dated April 2017 (ADAMS No. ML17130A222).
20. * [ ]
21. [ ]
22. [ ]
23. ASME Boiler and Pressure Vessel Code, Section II, Part D, "Materials - Properties", 2013 Edition.
24. [ ]
25. [ ]
26. [ ]
27. [ ]
28 U.S. NRC Regulatory Guide 1.99, Revision 2 "Radiation Embrittlement of Reactor Vessel Materials"

APPENDIX A: OPERATING STRESS ANALYSIS

A.1 Purpose

This appendix (Appendix A) is to describe development of the finite element (FE) model, the loads applied to FE model, and extracting stresses to support the fracture mechanics analysis presented in the main body of this document. Note that this appendix contains both Framatome/Babcock & Wilcox and Exelon/General Electric proprietary information.

A.2 Methodology

The methodology consists of:

1. Building an axially symmetric FE model which includes a section of the RV base material, a section of the original nozzle, the original J-groove weld, cladding, the new replacement nozzle, weld build-up and weld between replacement nozzle and weld build-up. The radius of the RV in the FE axi-symmetrical model was magnified for conservatism by 2.5 to account for difference in the membrane stresses between a sphere and cylinder of the same thickness and radius. There are two models with identical mesh: one for the thermal analysis and one for the structural analysis.
2. Applying the temperature and heat transfer coefficient of applicable transients for normal/upset (Heat Up/ Cool Down, Loss of [ ] Pump [ ] and Single Relief [Safety Valve Blowdown),] and emergency/faulted ([ ] Overpressure [ ]) conditions on the thermal FE model.
3. Defining the locations of interest for thermal gradients within the structure, obtaining values of thermal gradients for entire transient from runs on thermal model, and selecting the time points for structural runs.
4. Applying pressure and temperature on the structural model for the time points identified in the previous step to obtain stresses resulting from pressure and thermal gradients.
5. Defining two (2) stress classification lines across the thickness of the RV, one is near the nozzle opening; the second is away from discontinuity. Listing stress components at these stress classification path lines to support fracture mechanics analysis.

A.3 Assumptions and Modeling Simplifications

1. There are no unverified assumptions used within this appendix. Justified assumptions and modeling simplifications are detailed as follows.
2. Axially symmetric model is used to calculate result stresses. In order to account for difference in membrane and bending stresses of the cylindrical shell and spherical shell of the same radius and the wall thickness, the radius of the shell was magnified for conservatism by factor of 2.5. This value is based on experience with modeling similar geometries.
3. Geometry of the replacement nozzle is approximate. The inner radius of new nozzle is equal to inner radius of the original nozzle. Such approximation is acceptable since the area of interest is in the shell, far from the nozzle-to-weld pad weld.

4. Heat transfer coefficient inside shell is set to [ ] inside nozzle is set to [ ] These values are based on stress report values (document [ ] reference [1]). It is recognized that these values are applicable to the Feedwater Nozzle which is relatively distant from the instrumentation nozzle N16A, but is located in approximately the same flow conditions as feedwater nozzle, therefore the inside shell film coefficient can be used. The insulated surfaces of the nozzle and RV shell use film coefficient of [ ] Although other values can be justified, the difference is deemed insignificant for the purpose of this analysis, which is to provide stresses in the RV shell relatively far from the nozzle opening.
5. [

]
6. No external piping loads are considered in this appendix.

A.4 Design Inputs

The geometry of the model is based in part on information obtained from page A-55 (stress report [ ] reference [1]) and in part on drawing [ ] Shell Segment, drawing of nozzle repair, reference drawing [3], and reference drawing [22].

The thickness of the replacement nozzle and weld to new buildup in FE model is approximate. The difference between modeled and actual geometry is considered insignificant for the stresses in the section of the RV used for fracture mechanics analysis.

Material properties designation is based on reference drawing [3]. Reactor vessel shell is formed of SA-302 Grade B plates (nominal chemical composition Mn-½Mo) with inner surface cladded by stainless steel [ ] cladding (nominal chemical composition [ ]). The new weld pad buildup, repair nozzle and j-groove weld between repair nozzle and weld pad buildup are all of Inconel 690. These material designations can be found in Table A-1.

Table A-1: Material Designations

Item	Material Designation	Reference
Reactor Vessel, Base Material	SA-302 Grade B	[3] [22]
Reactor Vessel, Cladding	[ ]	
Original Nozzle	[ ]	
Original J-groove Weld	[ ]	
Repair Nozzle	[ ] UNS N06690 (Alloy 690)	
J-groove Weld to Repair Nozzle	Alloy 52M (Alloy 690)	
Weld Pad Build Up	Alloy 52M (Alloy 690)	

Figure A-1: Material Assignment

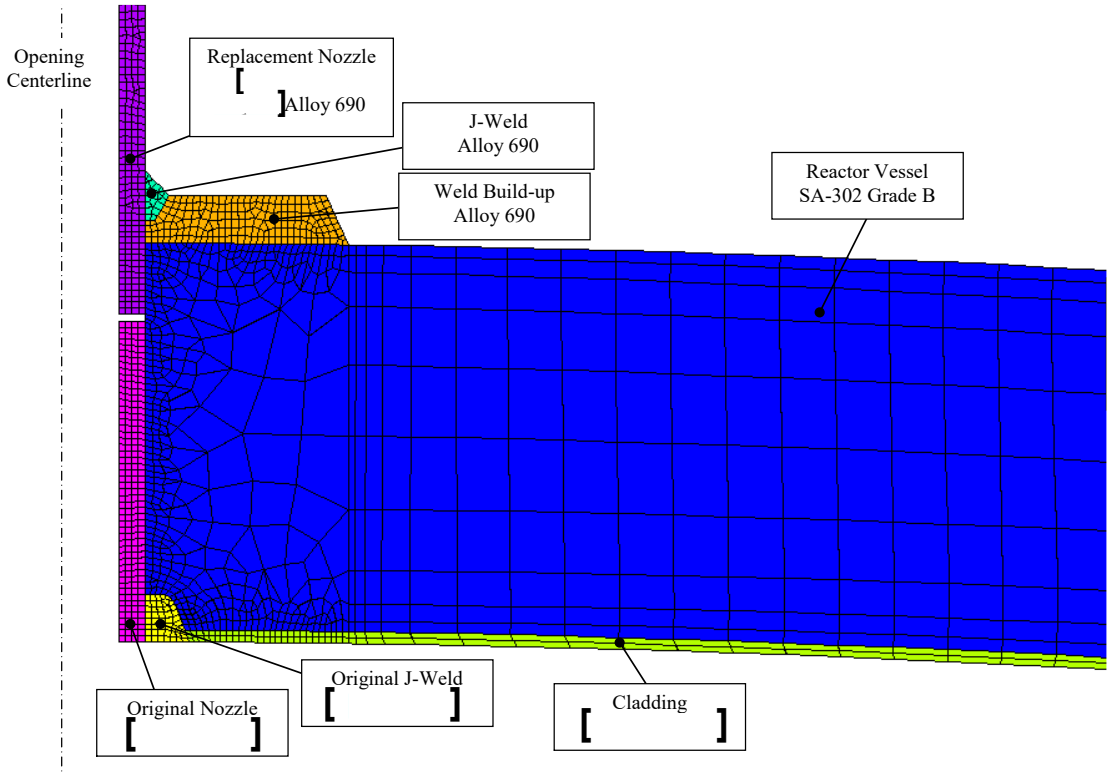

A.4.1 Design Conditions

Design conditions: pressure [ ] temperature [ ] ([ ] reference [1]).

A.4.2 Transient Definitions

Reference [18] is used extensively within this section. Unless stated otherwise, it is always pointing to drawing [ ] of reference [18] with MUR temperature and pressure updates defined in [ ] reference [1]. Such notation is used for better readability. Service levels are defined in TODI, Reference [21]. Four transients were considered in this evaluation:

1. HeatCool: [ ] This transient is designated as Normal/Upset Condition.
2. LossPmN: [ ] This transient is designated as Normal/Upset Condition. Note: transient with same name can be found in [ ] of reference [18], [ ] This transient was investigated but the results presented in the main body of this document use stresses developed from 'LossPmN' transient of reference [27].

3. OverPress: [ ] This transient is designated as Emergency/Faulted Condition.
4. SingRelf: [ ] This transient is designated as Normal/Upset Condition.

A heat transfer coefficient of [ ] is used on the RV shell inner surface, values of heat transfer coefficient of [ ] at the nozzle inner surface, and [ ] for the insulated condition on the model outer surfaces are considered appropriate in this location (see Section A.3).

Table A-2: Heat Up and Cool Down

Time [hour]	Temperature [°F]	Time [hour]	Pressure [psi]
[ ]			

Figure A-2: Heat Up and Cool Down

Table A-3: Loss of [ ] Pump, [ ]

Time [hour]	Temperature [°F]	Time [hour]	Pressure [psi]
[ ]			

Figure A-3: Loss of [ ] Pump, [ ]

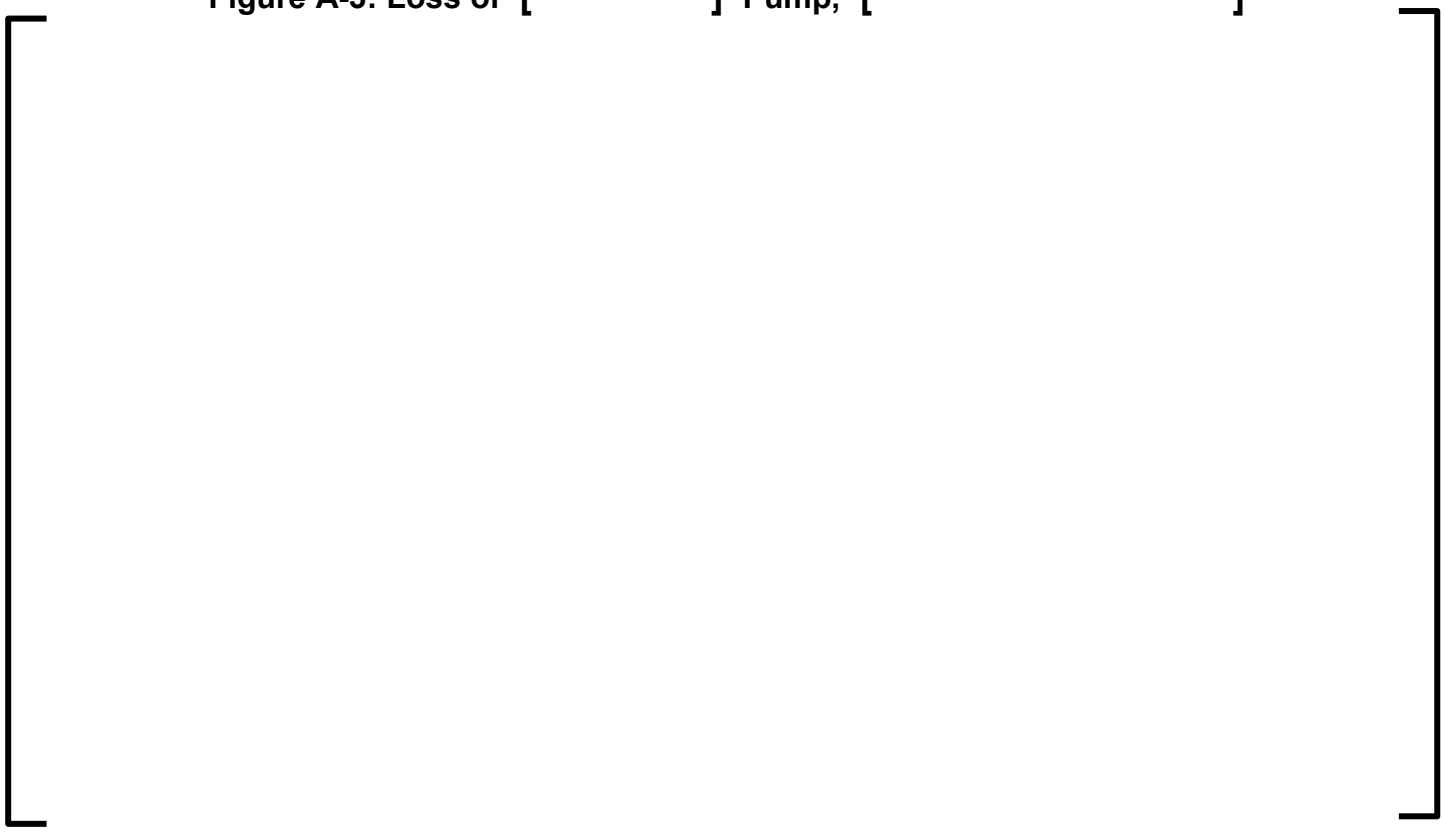

Table A-4: [ ] Overpressure [ ]

Time [hour]	Temperature [°F]	Time [hour]	Pressure [psi]
[			]

Figure A-4: [ ] Overpressure [ ]

Table A-5: Single Relief [ ]

Time [hour]	Temperature [°F]	Time [hour]	Pressure [psi]
[			]

Figure A-5: Single Relief [ ]

A.5 Calculations

Finite Element Model: The axially symmetric finite element model was built in ANSYS R19.2. The dimensions of the replacement nozzle are approximate.

A.5.1 Thermal Analysis

The temperatures listed in Table A-2 through Table A-5 were applied on all wetted surfaces. The outer surfaces of the replacement nozzle and the part of original nozzle inserted into the RV were thermally coupled with the inner surfaces of the opening bore. Input data for transient thermal analyses are listed in Section A.4.2. The thermal runs are documented in computer output files with names '*_thRun.out'.

A.5.2 Structural Analysis

The time-points for structural runs were selected based on the pressure transients (listed in Table A-2 through Table A-5) and thermal gradients (temperature differences) between locations of interest. The approximate location for thermal gradients can be found on Figure A-6. The thermal gradient listing can be found in computer files '*_dT.out'.

A list of time-points for which the structural runs were submitted can be found in the downstream calculations (Table C-1 through Table C-8 in Appendix C of this document). The pressure was applied on all wetted surfaces, including outer surface of original nozzle and inner surface of shell hole Figure A-8 (also shown on Figure A-7). Nodes on the outer edge of the shell were fixed in hoop direction, the cap force was applied for all structural runs on the end of replacement nozzle. The body temperature corresponding to the time of the transient is applied to the structural model from result file from thermal transient analysis of Section A.5.1. The structural runs are documented in computer files '*_stRun.out'.

Computer output file 'dCase_stRun.out' documents in the first load step the design case run.

Figure A-6: Locations for Thermal Gradients

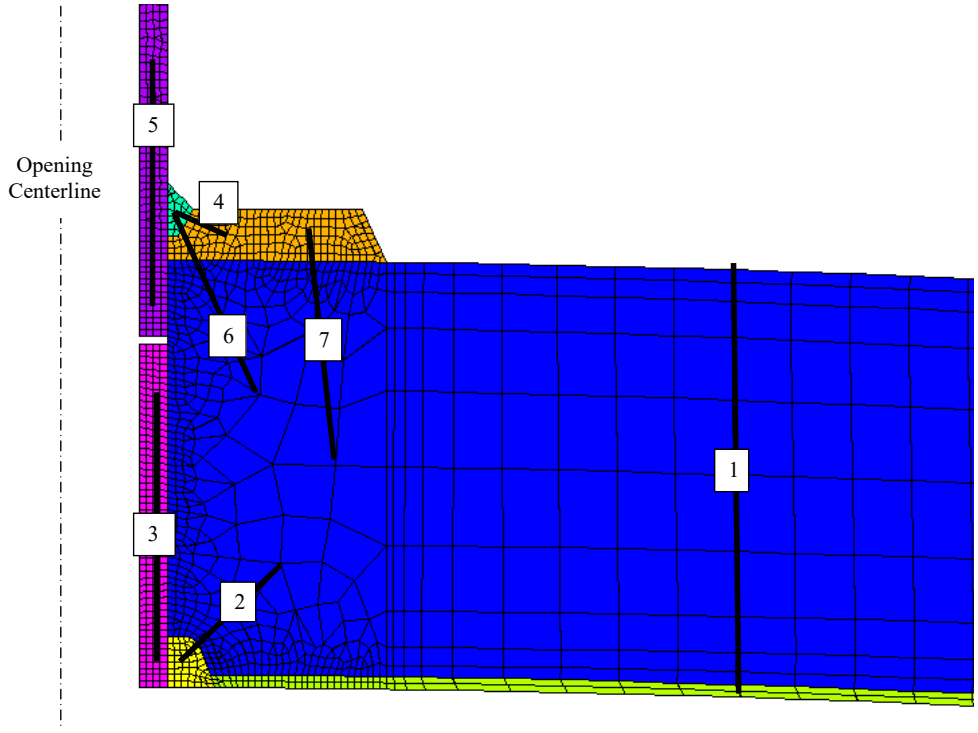

Figure A-7: FE Model, Crevice Boundary Conditions

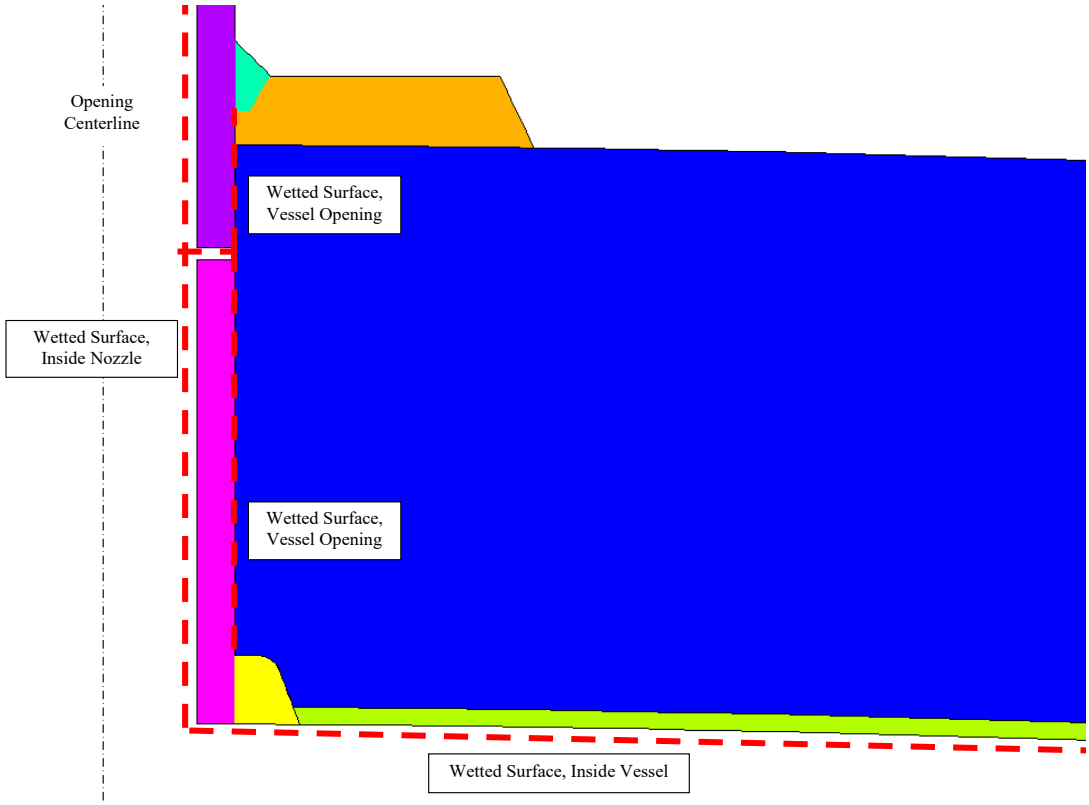

Figure A-8: Structural Run Boundary Conditions

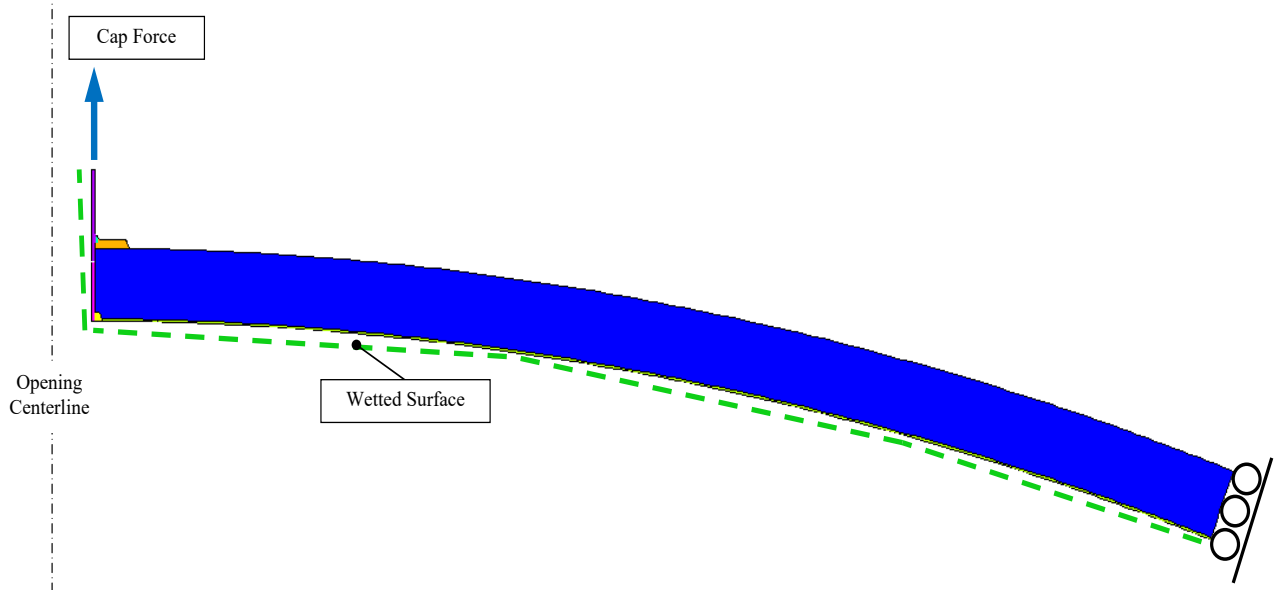

The computer output files '*_stPost.out' contains two formatted tables for each stress classification path line (shown on Figure A-9). Each '*_stPost.out' output file reports results for individual transients where the

summary table lists the transient time points, metal temperature at the location of original weld, along with membrane and bending hoop and axial component stresses at the stress classification line away from the opening discontinuity. Refer to the header of each table for the origin of stresses. Refer to Table A-6 for the description of listing as it appears in the applicable output file '*_stPost.out'.

Table A-6: Column Description

#	Item
1	table line number
2	time in the transient
3	temperature at location of original J-groove weld
4	axial membrane stress
5	axial bending stress, shell inner surface, 'bending I'
6	axial bending stress, shell outer surface, 'bending O'
7	hoop membrane stress
8	hoop bending stress, shell inner surface, 'bending I'
9	hoop bending stress, shell outer surface, 'bending O'

Stress components are listed in the cylindrical coordinate system with the RV shell centerline perpendicular to the display plane, hoop direction is the circumferential direction of entire RV shell, and radial direction is radial direction of entire RV shell. Also refer to Figure A-9 for approximate location of the stress classification lines 'NearPath' and 'FarPath.'.

Figure A-9: Results, Reported Locations

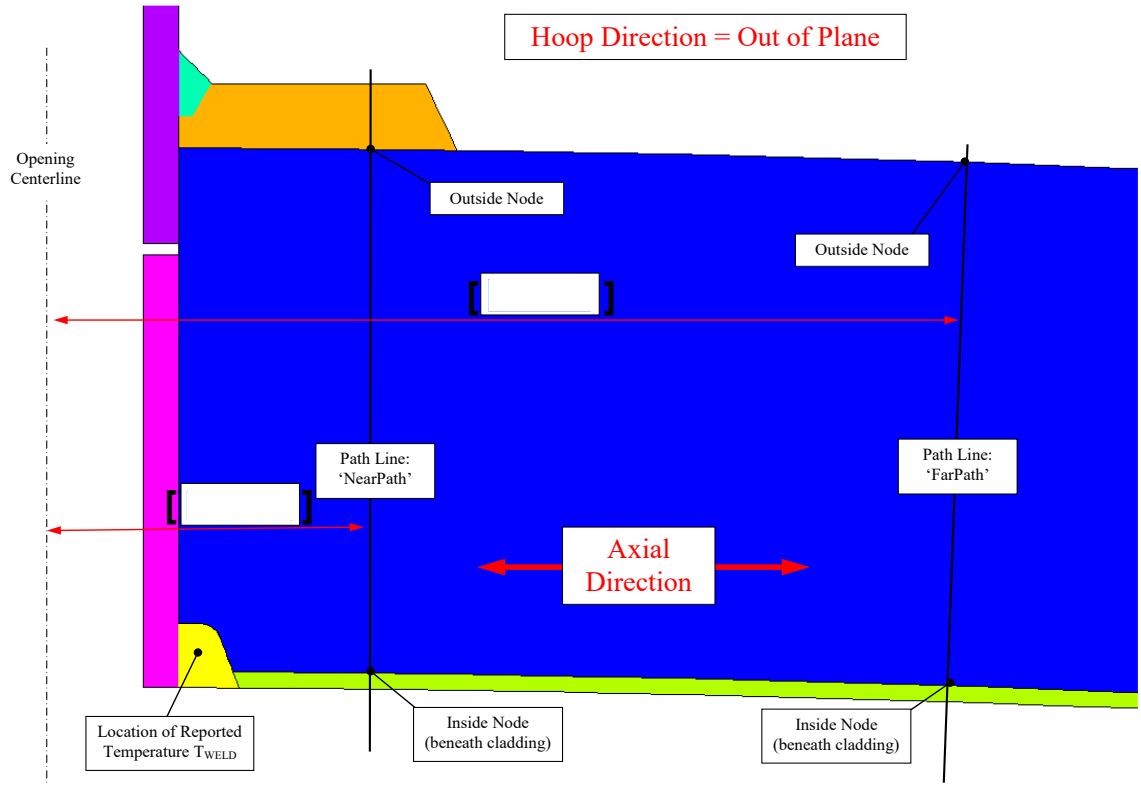

A.6 Computer Files

The computer files pertinent to revision 000 of this document Appendix A are located in ColdStor directory: '…/32-9321034-000/official/AppendixA'.

ANSYS Release 19.2 Mechanical Enterprise (latest EASI list version), Reference [16] was used for all FE runs documented herein. Use of this version of ANSYS is acceptable since error notices were reviewed and none was found applicable to this analysis.

Results of the calculations confirm that the inputs and structural responses of the models developed are within the range of applicability of ANSYS Mechanical Enterprise for these types of physical problems.

Computer runs were performed under controlled access of ANSYS Mechanical Enterprise, 19.2 on the approved platform "Lynchburg HPCv2". The computer used for this analysis is a multi-node server (auslynchpcc03), the computing nodes used to run this analysis were selected automatically by queuing handling software to be 'auslynchpc60' and 'auslynchpc59'. Queue number to run this job were 8327264 and 8329983 respectively. Jobs were submitted in interactive mode by Martin Kolar (preparer of revision 000).

The hardware platform for both nodes 'auslynchpc59' and 'auslynchpc60': [ ] operating system: Red Hat Enterprise Server release [ ]

Table A-7: List of Computer Files for Revision 000

crc	size (Byte)	modified date			time	file name
./official/AppendixA/01WbModel:						
07301	1186198	Nov	4	2020	18:36:33	PeachBottomN16.mesh.dat
53828	409125	Nov	4	2020	18:36:14	PeachBottomN16v0.wbpz
./official/AppendixA/02FeModel:						
38752	1489	Nov	3	2020	12:38:13	StructuralModel.mac
11455	2123	Nov	4	2020	21:08:06	ThermalModel.mac
./official/AppendixA/03TransientDefinitions:						
63588	1640	Nov	4	2020	15:18:54	HeatCool.mac
39021	1639	Nov	14	2020	9:34:54	LossPmpN.mac
30895	2677	Nov	4	2020	15:18:54	LossPump.mac
10336	1541	Nov	4	2020	15:18:54	OverPres.mac
29088	1032	Nov	4	2020	15:18:54	SingRelf.mac
./official/AppendixA/04TransientRuns:						
25710	40848	Nov	5	2020	22:47:03	DesignCase_stPost.out
56060	29630	Nov	5	2020	22:47:02	DesignCase_stRun.out
34926	95133	Nov	5	2020	22:48:02	HeatCool_dT.out
44118	183845	Nov	5	2020	22:48:12	HeatCool_stPost.out
52258	96772	Nov	5	2020	22:48:09	HeatCool_stRun.out
27239	322673	Nov	5	2020	22:48:00	HeatCool_thRun.out
12890	91366	Nov	5	2020	22:48:02	HeatCool_tr.parm
26985	73475	Nov	14	2020	10:09:38	LossPmpN_dT.out
44478	262495	Nov	14	2020	10:09:51	LossPmpN_stPost.out
54019	128585	Nov	14	2020	10:09:48	LossPmpN_stRun.out
41968	229478	Nov	14	2020	10:09:35	LossPmpN_thRun.out
13260	60909	Nov	14	2020	10:09:37	LossPmpN_tr.parm
56190	97047	Nov	5	2020	22:49:12	LossPump_dT.out
52902	355445	Nov	5	2020	22:49:31	LossPump_stPost.out
42378	167204	Nov	5	2020	22:49:27	LossPump_stRun.out
35666	364976	Nov	5	2020	22:49:09	LossPump_thRun.out
14645	95070	Nov	5	2020	22:49:12	LossPump_tr.parm
37167	22412	Nov	5	2020	22:49:46	OverPres_tr.parm
21341	45881	Nov	5	2020	22:49:47	OverPressure_dT.out
15381	205299	Nov	5	2020	22:49:58	OverPressure_stPost.out
26032	105624	Nov	5	2020	22:49:55	OverPressure_stRun.out
41107	111868	Nov	5	2020	22:49:44	OverPressure_thRun.out
14921	25839	Nov	5	2020	22:50:15	SingRelf_tr.parm
63243	48713	Nov	5	2020	22:50:16	SingleRelief_dT.out
18397	148099	Nov	5	2020	22:50:25	SingleRelief_stPost.out
42941	81505	Nov	5	2020	22:50:22	SingleRelief_stRun.out
20006	112139	Nov	5	2020	22:50:13	SingleRelief_thRun.out
63117	2925	Nov	5	2020	14:48:30	StressRun.mac
12137	1156	Nov	5	2020	21:01:35	ThermalRun.mac
26263	1091	Nov	5	2020	22:30:12	dCase_stRun.mac
./official/AppendixA/09ToolBoxFiles:						
08803	2393	Nov	13	2020	20:32:32	FractureData.mac
61043	7974	May	11	2017	19:36:45	MaterialProperties.mac
43018	7346	Nov	5	2020	22:46:04	dTpostProcessing.mac

APPENDIX B: SIF SOLUTION TEST CASES

The implementation of the SIF solution described in Section 2.1, from Reference [5], was tested to verify the implementation in the spreadsheet by reproducing Figures 10 (for tension) and 11 (for bending) of Reference [5]. The tension test case is shown in Figure B-1 and the bending test case is shown in Figure B-2. Open circles represent digitized data points from Reference [5] figures and solid lines are values calculated by the spreadsheet used in this report. The results show good agreement. The test cases are archived in the excel spreadsheet "*PeachBottom2_N16A_LEFM_EPFM_v1.xlsm*" and are stored in the ColdStor as described in Section 5.2.

Figure B-1: Test Case for Tension (Based on Figure 10 of [5])

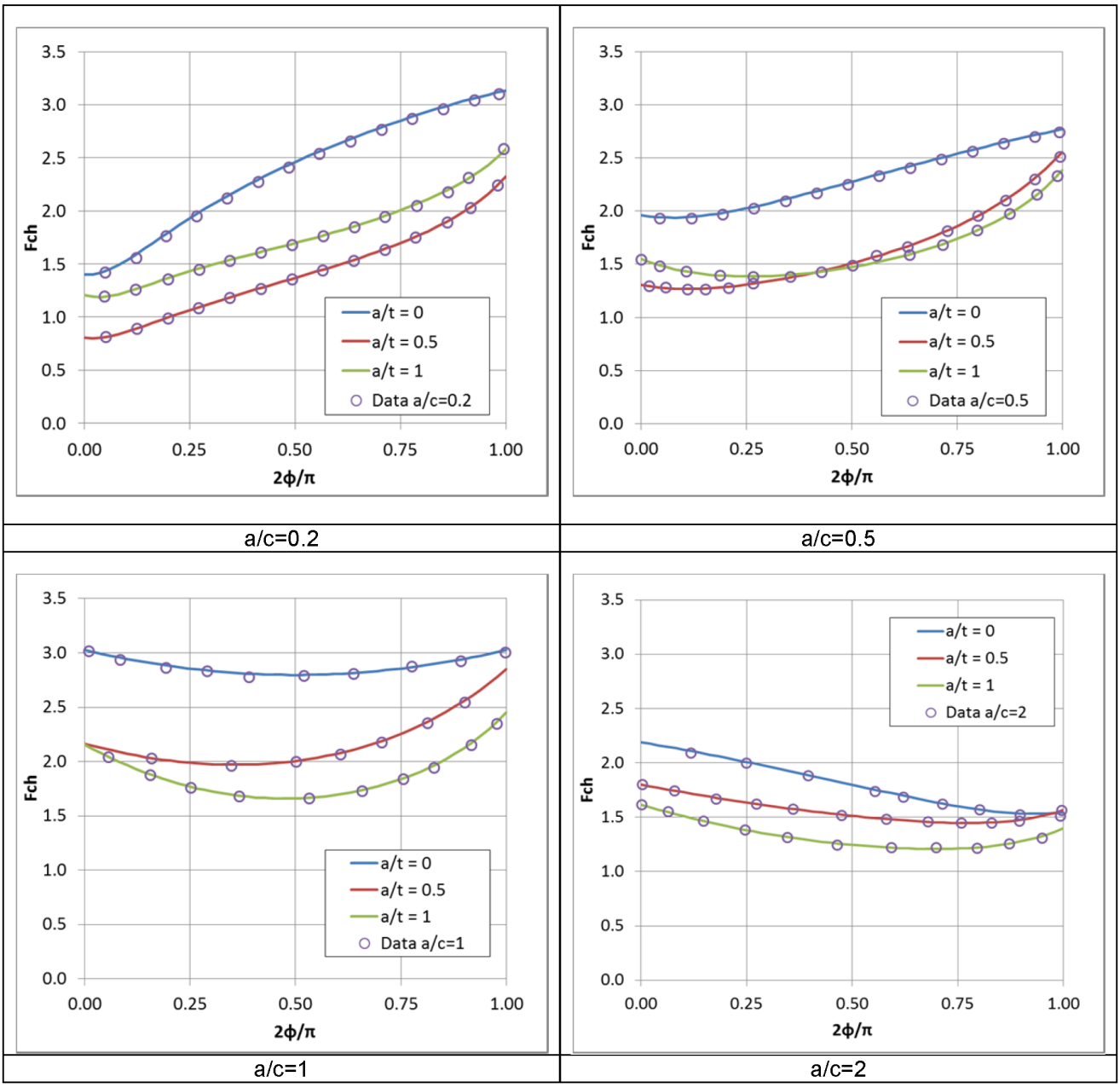

a/c=0.2 | a/c=0.5

a/c=1 | a/c=2

Figure B-2: Test Case for Bending (Based on Figure 11 of [5])

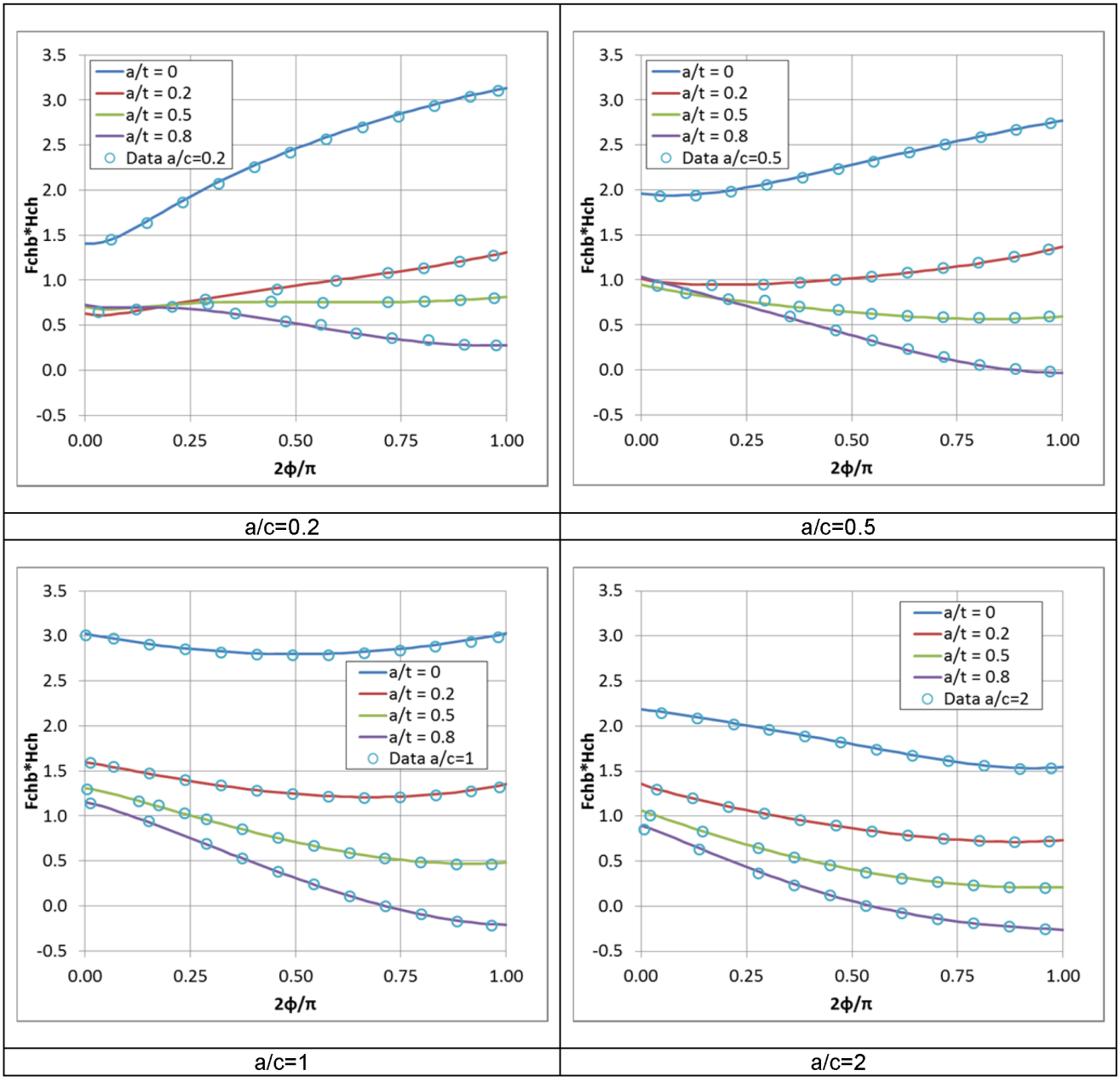

a/c=0.2 | a/c=0.5

a/c=1 | a/c=2

APPENDIX C: FM EVALUATION RESULT TABLES

Table C-1: LEFM Results – HUCD Transient

						note (1)			Membrane Stresses		Bending Stresses			Total Applied Stress		K		Plastic Zone		Plastic Zone Corrected K							
Transient	Service Level	Time	Pressure	Fluid Temperature	Metal Temperature	E	E'	σ_y	Pressure (pRi/t)	Crack Face Pressure	FE Model Bending	WRS	Crack Face Pressure	St	Sb	$\phi = 0^o$ K_I	$\phi = 90^o$ K_I	$\phi = 0^o$ r_y	$\phi = 90^o$ r_y	$\phi = 0^o$ K_{Ieff}	$\phi = 90^o$ K_{Ieff}	K_{IC}	K_{IC}/K $\phi = 0^o$	K_{IC}/K $\phi = 90^o$	Req'd Margin	LEFM Check?	LEFM/EPFM Applicable?
		hr	psig	°F	°F	ksi	ksi	ksi	ksi	ksi	ksi	ksi	ksi	ksi	ksi	ksi$\sqrt{in}$	ksi$\sqrt{in}$	in	in	ksi$\sqrt{in}$	ksi$\sqrt{in}$	ksi$\sqrt{in}$					
HUCD	Normal/Upset																									OK	LEFM Temperature Range
HUCD	Normal/Upset																									OK	LEFM Temperature Range
HUCD	Normal/Upset																									OK	LEFM Temperature Range
HUCD	Normal/Upset																									OK	EPFM Temperature Range
HUCD	Normal/Upset																									No Good	EPFM Temperature Range
HUCD	Normal/Upset																									No Good	EPFM Temperature Range
HUCD	Normal/Upset																									No Good	EPFM Temperature Range
HUCD	Normal/Upset																									No Good	EPFM Temperature Range
HUCD	Normal/Upset																									No Good	EPFM Temperature Range
HUCD	Normal/Upset																									No Good	EPFM Temperature Range
HUCD	Normal/Upset																									No Good	EPFM Temperature Range
HUCD	Normal/Upset																									OK	EPFM Temperature Range
HUCD	Normal/Upset																									OK	EPFM Temperature Range
HUCD	Normal/Upset																									OK	EPFM Temperature Range
HUCD	Normal/Upset																									OK	EPFM Temperature Range
HUCD	Normal/Upset																									OK	EPFM Temperature Range
HUCD	Normal/Upset																									OK	EPFM Temperature Range
HUCD	Normal/Upset																									OK	EPFM Temperature Range
HUCD	Normal/Upset																									OK	Transition Temperature Range
HUCD	Normal/Upset																									OK	LEFM Temperature Range
HUCD	Normal/Upset																									OK	LEFM Temperature Range
HUCD	Normal/Upset																									OK	LEFM Temperature Range

(1): Material properties at metal temperature.

Table C-2: LEFM Results – Loss of [ ] Pump Transient

						note (1)			Membrane Stresses		Bending Stresses			Total Applied Stress		K		Plastic Zone		Plastic Zone Corrected K						
Transient	Service Level	Time	Pressure	Fluid Temperature	Metal Temperature	E	E'	σ_y	Pressure (pRi/t)	Crack Face Pressure	FE Model Bending	WRS	Crack Face Pressure	St	Sb	$\phi = 0^o$ K_I	$\phi = 90^o$ K_I	$\phi = 0^o$ r_y	$\phi = 90^o$ r_y	$\phi = 0^o$ K_{Ieff}	$\phi = 90^o$ K_{Ieff}	K_{IC}	K_{IC}/K $\phi = 0^o$	K_{IC}/K $\phi = 90^o$	Req'd Margin	LEFM Check?	LEFM/EPFM Applicable?
		hr	psig	°F	°F	ksi	ksi	ksi	ksi	ksi	ksi	ksi	ksi	ksi	ksi	ksi√in	ksi√in	in	in	ksi√in	ksi√in	ksi√in	$\phi = 0^o$	$\phi = 90^o$			
Loss of Pump	Normal/Upset																									No Good	EPFM Temperature Range

Table C-3: LEFM Results – [ ] Overpressure [ ] Transient

						note (1)			Membrane Stresses		Bending Stresses			Total Applied Stress		K		Plastic Zone		Plastic Zone Corrected K						
Transient	Service Level	Time	Pressure	Fluid Temperature	Metal Temperature	E	E'	σ_y	Pressure (pRi/t)	Crack Face Pressure	FE Model Bending	WRS	Crack Face Pressure	St	Sb	$\phi = 0°$ K_I	$\phi = 90°$ K_I	$\phi = 0°$ r_y	$\phi = 90°$ r_y	$\phi = 0°$ K_{Ieff}	$\phi = 90°$ K_{Ieff}	K_{IC}	K_{IC}/K $\phi = 0°$	K_{IC}/K $\phi = 90°$	Req'd Margin	LEFM Check?	LEFM/EPFM Applicable?
		hr	psig	°F	°F	ksi	ksi	ksi	ksi	ksi	ksi	ksi	ksi	ksi	ksi	ksi√in	ksi√in	in	in	ksi√in	ksi√in	ksi√in	$\phi = 0°$	$\phi = 90°$			
Over Pressure	Emergency/Faulted																									OK	EPFM Temperature Range
Over Pressure	Emergency/Faulted																									OK	EPFM Temperature Range
Over Pressure	Emergency/Faulted																									OK	EPFM Temperature Range
Over Pressure	Emergency/Faulted																									OK	EPFM Temperature Range
Over Pressure	Emergency/Faulted																									OK	EPFM Temperature Range
Over Pressure	Emergency/Faulted																									OK	EPFM Temperature Range
Over Pressure	Emergency/Faulted																									OK	EPFM Temperature Range
Over Pressure	Emergency/Faulted																									OK	EPFM Temperature Range
Over Pressure	Emergency/Faulted																									OK	EPFM Temperature Range
Over Pressure	Emergency/Faulted																									OK	EPFM Temperature Range
Over Pressure	Emergency/Faulted																									OK	EPFM Temperature Range
Over Pressure	Emergency/Faulted																									OK	EPFM Temperature Range
Over Pressure	Emergency/Faulted																									OK	EPFM Temperature Range
Over Pressure	Emergency/Faulted																									OK	EPFM Temperature Range
Over Pressure	Emergency/Faulted																									OK	EPFM Temperature Range
Over Pressure	Emergency/Faulted																									OK	EPFM Temperature Range
Over Pressure	Emergency/Faulted																									OK	EPFM Temperature Range
Over Pressure	Emergency/Faulted																									OK	EPFM Temperature Range
Over Pressure	Emergency/Faulted																									OK	EPFM Temperature Range
Over Pressure	Emergency/Faulted																									OK	EPFM Temperature Range
Over Pressure	Emergency/Faulted																									OK	EPFM Temperature Range
Over Pressure	Emergency/Faulted																									OK	EPFM Temperature Range
Over Pressure	Emergency/Faulted																									OK	EPFM Temperature Range
Over Pressure	Emergency/Faulted																									OK	EPFM Temperature Range
Over Pressure	Emergency/Faulted																									OK	EPFM Temperature Range
Over Pressure	Emergency/Faulted																									OK	EPFM Temperature Range
Over Pressure	Emergency/Faulted																									OK	EPFM Temperature Range

(1): Material properties at metal temperature.

Table C-4: LEFM Results – Single Relief [ ] Transient

						note (1)			Membrane Stresses		Bending Stresses			Total Applied Stress		K		Plastic Zone		Plastic Zone Corrected K							
Transient	Service Level	Time	Pressure	Fluid Temperature	Metal Temperature	E	E'	σ_y	Pressure (pRi/t)	Crack Face Pressure	FE Model Bending	WRS	Crack Face Pressure	St	Sb	$\phi = 0^o$ K_I	$\phi = 90^o$ K_I	$\phi = 0^o$ r_y	$\phi = 90^o$ r_y	$\phi = 0^o$ K_{Ieff}	$\phi = 90^o$ K_{Ieff}	K_{IC}	K_{IC}/K $\phi = 0^o$	K_{IC}/K $\phi = 90^o$	Req'd Margin	LEFM Check?	LEFM/EPFM Applicable?
		hr	psig	°F	°F	ksi	ksi	ksi	ksi	ksi	ksi	ksi	ksi	ksi	ksi	ksi√in	ksi√in	in	in	ksi√in	ksi√in	ksi√in	$\phi = 0^o$	$\phi = 90^o$			
Single Relief	Normal/Upset																									No Good	EPFM Temperature Range
Single Relief	Normal/Upset																									No Good	EPFM Temperature Range
Single Relief	Normal/Upset																									No Good	EPFM Temperature Range
Single Relief	Normal/Upset																									No Good	EPFM Temperature Range
Single Relief	Normal/Upset																									No Good	EPFM Temperature Range
Single Relief	Normal/Upset																									No Good	EPFM Temperature Range
Single Relief	Normal/Upset																									No Good	EPFM Temperature Range
Single Relief	Normal/Upset																									No Good	EPFM Temperature Range
Single Relief	Normal/Upset																									No Good	EPFM Temperature Range
Single Relief	Normal/Upset																									No Good	EPFM Temperature Range
Single Relief	Normal/Upset																									No Good	EPFM Temperature Range
Single Relief	Normal/Upset																									No Good	EPFM Temperature Range
Single Relief	Normal/Upset																									No Good	EPFM Temperature Range
Single Relief	Normal/Upset																									No Good	EPFM Temperature Range
Single Relief	Normal/Upset																									OK	EPFM Temperature Range
Single Relief	Normal/Upset																									OK	Transition Temperature Range
Single Relief	Normal/Upset																									OK	LEFM Temperature Range
Single Relief	Normal/Upset																									OK	LEFM Temperature Range

(1): Material properties at metal temperature.

Table C-5: EPFM Results (Section 3.1 of CC N-749) – HUCD Transient

Transient	Service Level	Time	St	Sb-Sb$_{WRS}$	$\phi = 0^o$ K$_{Ip}$	$\phi = 0^o$ K$_{Is}$	$\phi = 90^o$ K$_{Ip}$	$\phi = 90^o$ K$_{Is}$	Plastic Zone $\phi = 0^o$ r$_y$	Plastic Zone $\phi = 90^o$ r$_y$	Plastic Zone Corrected K $\phi = 0^o$ K$_{Ip}$	Plastic Zone Corrected K $\phi = 0^o$ K$_{Is}$	Plastic Zone Corrected K $\phi = 90^o$ K$_{Ip}$	Plastic Zone Corrected K $\phi = 90^o$ K$_{Is}$	$\phi = 0^o$ J$_{app}$	$\phi = 90^o$ J$_{app}$	CVN = [ ] J$_{0.1}$	J$_{app}$/J$_{0.1}$	EPFM Check?
		hr	ksi	ksi	ksi√in	ksi√in	ksi√in	ksi√in	in	in	ksi√in	ksi√in	ksi√in	ksi√in	kips/in	kips/in	kips/in		
HUCD	Normal/Upset																		< 1, OK
HUCD	Normal/Upset																		< 1, OK
HUCD	Normal/Upset																		< 1, OK
HUCD	Normal/Upset																		< 1, OK
HUCD	Normal/Upset																		< 1, OK
HUCD	Normal/Upset																		< 1, OK
HUCD	Normal/Upset																		< 1, OK
HUCD	Normal/Upset																		< 1, OK
HUCD	Normal/Upset																		< 1, OK
HUCD	Normal/Upset																		< 1, OK
HUCD	Normal/Upset																		< 1, OK
HUCD	Normal/Upset																		< 1, OK
HUCD	Normal/Upset																		< 1, OK
HUCD	Normal/Upset																		< 1, OK
HUCD	Normal/Upset																		< 1, OK
HUCD	Normal/Upset																		< 1, OK
HUCD	Normal/Upset																		< 1, OK
HUCD	Normal/Upset																		< 1, OK
HUCD	Normal/Upset																		< 1, OK
HUCD	Normal/Upset																		< 1, OK
HUCD	Normal/Upset																		< 1, OK
HUCD	Normal/Upset																		< 1, OK
HUCD	Normal/Upset																		< 1, OK
HUCD	Normal/Upset																		< 1, OK
HUCD	Normal/Upset																		< 1, OK
HUCD	Normal/Upset																		< 1, OK
HUCD	Normal/Upset																		< 1, OK
HUCD	Normal/Upset																		< 1, OK

*Temperatures at these time points are below T_{cI}, results are for information only.

Table C-6: EPFM Results (Section 3.1 of CC N-749) – Loss of [ ] Pump Transient

									Plastic Zone		Plastic Zone Corrected K								
					$\phi = 0^o$	$\phi = 0^o$	$\phi = 90^o$	$\phi = 90^o$	$\phi = 0^o$	$\phi = 90^o$	$\phi = 0^o$	$\phi = 0^o$	$\phi = 90^o$	$\phi = 90^o$	$\phi = 0^o$	$\phi = 90^o$	CVN = [ ]		
Transient	Service Level	Time	St	$Sb\text{-}Sb_{WRS}$	K_{Ip}	K_{Is}	K_{Ip}	K_{Is}	r_y	r_y	K_{Ip}	K_{Is}	K_{Ip}	K_{Is}	J_{app}	J_{app}	$J_{0.1}$	$J_{app}/J_{0.1}$	EPFM Check?
		hr	ksi	ksi	ksi√in	ksi√in	ksi√in	ksi√in	in	in	ksi√in	ksi√in	ksi√in	ksi√in	kips/in	kips/in	kips/in		
Loss of Pump	Normal/Upset	[																	< 1, OK
Loss of Pump	Normal/Upset

Table C-7: EPFM Results (Section 3.1 of CC N-749) – [ ] Overpressure [ ] Transient

									Plastic Zone		Plastic Zone Corrected K								
					$\phi = 0^o$	$\phi = 0^o$	$\phi = 90^o$	$\phi = 90^o$	$\phi = 0^o$	$\phi = 90^o$	$\phi = 0^o$	$\phi = 0^o$	$\phi = 90^o$	$\phi = 90^o$	$\phi = 0^o$	$\phi = 90^o$	CVN = [ ]		
Transient	Service Level	Time	St	$Sb\text{-}Sb_{WRS}$	K_{Ip}	K_{Is}	K_{Ip}	K_{Is}	r_y	r_y	K_{Ip}	K_{Is}	K_{Ip}	K_{Is}	J_{app}	J_{app}	$J_{0.1}$	$J_{app}/J_{0.1}$	EPFM Check?
		hr	ksi	ksi	ksi√in	ksi√in	ksi√in	ksi√in	in	in	ksi√in	ksi√in	ksi√in	ksi√in	kips/in	kips/in	kips/in		
Over Pressure	Emergency/Faulted	[																	< 1, OK
Over Pressure	Emergency/Faulted

Table C-8: EPFM Results (Section 3.1 of CC N-749) – Single Relief [ ] Transient

Transient	Service Level	Time	St	Sb-Sb$_{WRS}$	$\phi = 0^o$ K_{Ip}	$\phi = 0^o$ K_{Is}	$\phi = 90^o$ K_{Ip}	$\phi = 90^o$ K_{Is}	Plastic Zone $\phi = 0^o$ r_y	Plastic Zone $\phi = 90^o$ r_y	Plastic Zone Correction K $\phi = 0^o$ K_{Ip}	Plastic Zone Correction K $\phi = 0^o$ K_{Is}	Plastic Zone Correction K $\phi = 90^o$ K_{Ip}	Plastic Zone Correction K $\phi = 90^o$ K_{Is}	$\phi = 0^o$ J_{app}	$\phi = 90^o$ J_{app}	CVN = [ ] $J_{0.1}$	$J_{app}/J_{0.1}$	EPFM Check?
		hr	ksi	ksi	ksi√in	ksi√in	ksi√in	ksi√in	in	in	ksi√in	ksi√in	ksi√in	ksi√in	kips/in	kips/in	kips/in		
Single Relief	Normal/Upset	[																	< 1, OK
Single Relief	Normal/Upset

Attachment 6

"Peach Bottom 2 N16A Instrument Nozzle Repair Stress One-Cycle Justification Non-Proprietary," Document Number 32- 9321035–001 (Non-Proprietary Version)

framatome

CALCULATION SUMMARY SHEET (CSS)

Document No. 32 - 9321035 - 001 Safety Related: ☒Yes ☐ No

Title Peach Bottom 2 N16A Instrument Nozzle Repair Stress One-Cycle Justification Non-Proprietary

PURPOSE AND SUMMARY OF RESULTS:

PURPOSE:

The purpose of this calculation is to justify the operation of Peach Bottom Unit 2 with a repaired Instrumentation Nozzle (N16A) for one operating cycle.

Rev. 001: The proprietary version is updated; accordingly the non-proprietary version is updated.

RESULTS:

The Instrumentation Nozzle repair satisfies the applicable ASME Code requirements for one operating cycle.

Rev. 001: No changes to the calculation.

This is the non-proprietary version of Framatome Document 32-9321033-003.

If the computer software used herein is not the latest version per the EASI list, AP 0402-01 requires that justification be provided.

THE FOLLOWING COMPUTER CODES HAVE BEEN USED IN THIS DOCUMENT:

CODE/VERSION/REV	CODE/VERSION/REV
None	

THE DOCUMENT CONTAINS ASSUMPTIONS THAT SHALL BE VERIFIED PRIOR TO USE

☐Yes

☒ No

Review Method: ☒ Design Review (Detailed Check)

☐ Alternate Calculation

Does this document establish design or technical requirements? ☐ YES ☒ NO

Does this document contain Customer Required Format? ☐ YES ☒ NO

Signature Block

Name and Title (printed or typed)	Signature	P/R/A/M and LP/LR	Date	Pages/Sections Prepared/Reviewed/Approved
Kaihong Wang, Advisory Engineer	*K WANG 11/19/2020*	P		All.
Tomas Straka, Advisory Engineer	*T STRAKA 11/19/2020*	R		All.
David Cofflin, Supervisory Engineer	*D KIM for DR COFFLIN 11/19/2020*	A		All.

Notes: P/R/A designates Preparer (P), Reviewer (R), Approver (A);
LP/LR designates Lead Preparer (LP), Lead Reviewer (LR);
M designates Mentor (M)

In preparing, reviewing and approving revisions, the lead preparer/reviewer/approver shall use 'All' or 'All except ___' in the pages/sections reviewed/approved. 'All' or 'All except ___' means that the changes and the effect of the changes on the entire document have been prepared/reviewed/approved. It does not mean that the lead preparer/reviewer/approver has prepared/reviewed/approved all the pages of the document.

With Approver permission, calculations may be revised without using the latest CSS form. This deviation is permitted when expediency and/or cost are a factor. Approver shall add a comment in the right-most column that acknowledges and justifies this deviation.

Project Manager Approval of Customer References and/or Customer Formatting (N/A if not applicable)

Name (printed or typed)	Title (printed or typed)	Signature	Date	Comments
N/A	N/A	N/A	N/A	N/A

Record of Revision

Revision No.	Pages/Sections/Paragraphs Changed	Brief Description / Change Authorization
000	All	Original release
001	Pages 1-6	Revised for Rev. 001.
	Pages 7-18	Updated to be consistent with the proprietary version.

Engineering Certification

The seal of the Professional Engineer applied to this page signifies that this calculation has been prepared under the responsible charge of the Professional Engineer. This document was created to satisfy the structural analysis portion of Section 5.4 of Reference [1], requiring demonstration that requirements of Reference [2] are satisfied. This document does not constitute a Certified Design Report for the full lifetime of the repair.

I, hereby, certify to the best of my knowledge and belief that the analysis herein is correct and complete with respect to its stated purpose.

Printed Name: Don Kim

Title: Advisory Engineer

Signature: 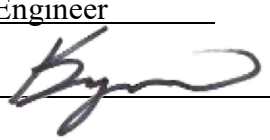 Date: 11/19/2020

State: VA License No.: 0402041365 Expiration Date: 7/31/2022

Seal:

Table of Contents

Page

SIGNATURE BLOCK 2

RECORD OF REVISION 3

ENGINEERING CERTIFICATION 4

LIST OF TABLES 6

1.0 INTRODUCTION 7

2.0 PURPOSE AND SCOPE 7

3.0 ANALYTICAL METHODOLOGY 7

4.0 ASSUMPTIONS 7

4.1 Unverified Assumptions 7

4.2 Justified Assumptions 8

5.0 CALCULATIONS 8

5.1 Primary Stress Evaluation 8

5.1.1 Loading 8

5.1.2 Primary Stress Calculation 9

5.2 Interference Check 16

5.3 Secondary and Peak Stresses 16

5.4 Corrosion Evaluation 17

6.0 COMPUTER USAGE 17

7.0 CONCLUSION 18

8.0 REFERENCES 18

List of Tables

Page

Table 5-1: Local Piping Loads at Pipe-to-Coupling Weld 9
Table 5-2: Local Piping Loads Under Service Levels at Pipe-to-Coupling Weld 9
Table 5-3: J-groove Weld Cross-Sectional Property 11
Table 5-4: Stress Intensity on J-groove Weld with Level D Loads (Pressure and Piping Loads) 11
Table 5-5: Stress Intensity on J-groove Weld due to Pressure Only 12
Table 5-6: Stress Intensity on Replacement Nozzle with Level D Loads (Pressure and Piping Loads) 13
Table 5-7: Stress Intensity on Replacement Nozzle due to Pressure Only 14

1.0 INTRODUCTION

The Instrumentation Nozzle (N16A) was found to be leaking at the Peach Bottom Unit 2. A half-nozzle repair is being performed per Reference [1].

Nozzle N16A is located in shell [ ] plant elevation or [ ] above the inside surface of the bottom of the reactor vessel (RV) (Reference [1]). The original nozzle is connected to the vessel wall with a partial penetration J-groove weld made on the inside of the reactor vessel (RV). The repair utilized the half-nozzle approach to modify the original nozzle. The half-nozzle approach replaces the outer portion of the existing nozzle with a new Alloy 690 nozzle and establishes a new pressure boundary on the outside surface of the RV shell with a partial penetration J-groove weld in a new Alloy 52M weld pad. The remnant of the original nozzle remains in place, along with the original J-groove weld. The original [ ] nozzle and the stainless steel safe end are replaced with an Alloy 690 nozzle connected to a stainless steel reducing coupling.

2.0 PURPOSE AND SCOPE

This calculation justifies plant operation for one cycle with the repaired nozzle, based on the requirements of the ASME Code (Reference [2]). A subsequent analysis will demonstrate acceptability of the repaired nozzle for operation beyond one cycle.

Per Reference [1], the scope of this analysis includes the modification (new weld pad, new J-groove weld, replacement nozzle) up to the terminal end of the replacement nozzle. The reducing coupling as well as the fillet weld between the coupling and the nozzle end is outside the scope of this analysis.

Rev. 001: The J-groove weld bore size is increased on-site to remove some PT indications (Reference [13]). As a result, both ID and OD of the nozzle near the J-groove weld are increased. The calculation is updated to address the repair deviation from the design, and the as-measured dimensions are used where applicable.

3.0 ANALYTICAL METHODOLOGY

The following steps will be performed to demonstrate the acceptability of the half-nozzle repair:

- Acceptability of the new J-groove weld configuration with respect to ASME Code dimensional requirements will be determined.
- Primary stress criteria will be evaluated.
- An assessment of the secondary and peak stresses, and fatigue will be made, with regard to a single cycle of operation.

Methodology for the calculation of required area of reinforcement is provided in Section 5.1.2.4.

4.0 ASSUMPTIONS

4.1 Unverified Assumptions

There is no unverified assumption used in this calculation.

4.2 Justified Assumptions

1) [

]

2) [

]

5.0 CALCULATIONS

5.1 Primary Stress Evaluation

The purpose of this section is to verify the primary stress requirements are met for the design shown in Reference [3]. The replacement nozzle is shown in Reference [4]. The verification is based on the requirements of Reference [2] and as specified in Reference [1]. More specifically the following are evaluated in the one cycle justification:

1) Partial penetration J-groove weld (Alloy 52M)
2) New nozzle (Alloy 690)
3) New weld pad (Alloy 52M)
4) Stresses in the vicinity of the opening (Low alloy steel, done by reinforcement check)

5.1.1 Loading

The external mechanical loadings are specified in Reference [5]. The maximum internal pressure of [ ] psi occurs during the Hydrostatic Test as specified in Reference [6]. Based on Reference [5], the external loads are applied at the weld between the 1-1/2″ pipe and the 2″x1-1/2″ reducing coupling. It is located [ ] from the outside surface of the RV base metal, where [ ] is the distance from the RV outside surface to the nozzle end weld as shown in Reference [3] and [ ] is the height of the coupling (Reference [7]). Applicable loads from Reference [5] are collected in Table 5-1 where the direction A is the nozzle axial positive outwards, B is vertical positive up and C is determined by the right hand rule.

Table 5-1: Local Piping Loads at Pipe-to-Coupling Weld

Load Case	F_A, lbs	F_B, lbs	F_C, lbs	M_A, ft-lbs	M_B, ft-lbs	M_C, ft-lbs
WT01	[					]
THRM01						
SAMOU						
SAMSS						
SEISOB						
SEISDB						

The load combinations are specified in Reference [5]. No Level C (Emergency) conditions are specified for the instrumentation nozzle in Reference [5]. For the purpose of primary stress evaluation, the load combinations are listed as follows:

Level A and B: [
]

Level D: [ ]

Piping loads at the pipe-to-coupling weld for different service levels are calculated conservatively as the summation of absolute values, as collected in Table 5-2 where directions x, y and z are the directions A, B and C in Table 5-1, respectively.

Table 5-2: Local Piping Loads Under Service Levels at Pipe-to-Coupling Weld

Service Load	F_x, lbs	F_y, lbs	F_z, lbs	M_x, in-lbs	M_y, in-lbs	M_z, in-lbs
Level A&B	[					]
Level D						

5.1.2 Primary Stress Calculation

Loads listed in Table 5-2 are used to calculate stresses at locations of interest using the following equations:

Axial stress: $$\sigma_x = \frac{PR_i^2}{R_o^2 - R_i^2} + \frac{(M_b + F_s L)R}{I} + \frac{F_x}{A} \quad (1)$$

Hoop stress: $$\sigma_y = \frac{PR_i^2}{R_o^2 - R_i^2}\left(\frac{R_o^2}{R^2} + 1\right) \quad (2)$$

Radial stress: $$\sigma_z = -\frac{PR_i^2}{R_o^2 - R_i^2}\left(\frac{R_o^2}{R^2} - 1\right) \quad (3)$$

Shear stresses: $$\tau_{xy} = \frac{M_x R}{J} + \frac{F_s}{A}, \tau_{yz} = \tau_{xz} = 0 \quad (4)$$

where,

P = maximum pressure, [ ]

R_i = Cross section inner radius, in.

R_o = Cross section outer radius, in.

M_b = bending moment, in-lbs, = $\sqrt{M_y^2 + M_z^2}$

M_x = torsional moment, in-lbs

F_x = axial load, lbs

F_s = shear load, lbs, = $\sqrt{F_y^2 + F_z^2}$

L = moment arm distance, in.

R = distance from centroid to section at which stresses are computed, in.

$I = \frac{\pi}{4}(R_o^4 - R_i^4)$, area moment of inertia, in^4.

J = 2I, polar moment of inertia, in^4.

$A = \pi(R_o^2 - R_i^2)$, cross sectional area, in^2.

Solving the following equation for the three principal stresses $\sigma_1, \sigma_2, \sigma_3$:

$$\sigma^3 - (\sigma_x + \sigma_y + \sigma_z)\sigma^2 + (\sigma_x\sigma_y + \sigma_y\sigma_z + \sigma_x\sigma_z - \tau_{xy}^2 - \tau_{yz}^2 - \tau_{xz}^2)\sigma - \sigma_x\sigma_y\sigma_z - 2\tau_{xy}\tau_{yz}\tau_{xz} + \sigma_x\tau_{yz}^2 + \sigma_y\tau_{xz}^2 + \sigma_z\tau_{xy}^2 = 0 \quad (5)$$

Stress intensity (SI) is then: SI = $\max(|\sigma_1 - \sigma_2|, |\sigma_2 - \sigma_3|, |\sigma_1 - \sigma_3|)$.

For the primary stress calculation, the level D loads are used conservatively to calculate stresses that are compared to the allowable stress values for level A (i.e., S_m for P_m, $1.5S_m$ for P_L+P_b). The allowable stress intensity S_m for Alloy 52M and Alloy 690 at 575°F is 23.3 ksi, Reference [8]. The primary stresses are calculated at the inner radius, mean radius and outer radius. The mean radius location is used to check the primary membrane limit. The maximum stress from the outer and inner radii is used to check the primary membrane plus bending limit. The mean radius is calculated using the following equation $(R_o+R_i)/2$.

In the following calculation, moment arm L = [ ] (as aforementioned which included the weld pad thickness) is conservatively used in calculating stresses on the new J-groove weld; moment arm L = [ ] (distance between the nozzle end and the pipe-to-coupling weld) is used in calculating stresses on the nozzle end considering the distance between the nozzle end and the original pipe-to-coupling weld. The J-groove weld is finally machined to have an oversized bore as shown in Step 5.4 of Reference [3] to remove some PT indications. The as-measured bore size is [ ] (two measurements taken) per Reference [13]. Accordingly, the replacement nozzle is machined by the "final contingency machining" shown in Reference [4]. The as-measured nozzle OD for the J-groove is [ ] (Reference [13]).

5.1.2.1 New J-Groove Weld

Weld Size (NB-3352.4, Reference [2])

This weld needs to satisfy the minimum dimension requirements of FIG. NB-4244(d)-1(e) and NB-3352.4(d)(2).

With the nozzle wall thickness t_n = [ ] (References [13] and [4], considering also the nozzle ID tolerance):

The minimum value: $t_c = \min(0.7t_n, 0.25) = \min(0.7*$ [ ] $0.25) = 0.25''$. The actual value of t_c is conservatively estimated to be: [ ] > 0.25″. This requirement is satisfied.

The fillet leg and the J-groove depth shall be no less than ¾ t_n = 0.75* [ ] The actual J-groove depth value is [ ] and the fillet leg is [ ] This requirement is satisfied.

The weld length along the nozzle OD shall be no less than 1.5t_n = 1.5* [ ] The actual value is [ ] minimum. This requirement is satisfied.

The gap between the nozzle end and the counter bore surface shall be in the range of [ ] and t_n [ ] The actual value is between [ ] This requirement is satisfied.

Nozzle Diametric Clearance (NB-3337.3(a), Reference [2])

For a nozzle OD between 1" and 4" the maximum diametric clearance of 0.020 per NB-3337.3(a) is satisfied with the as-measured dimensions (Reference [13]): [ ] (nozzle OD), [ ] (bore ID max.), diametric clearance = [ ]

Stress Intensity (SI)

Stress intensities on the J-groove weld due to combined loads (pressure, piping loads) are calculated based on the weld throat section, with the R_i and R_o determined as follows.

R_i = (Nozzle OD)/2

R_o = [Nozzle OD +$\sqrt{2}$*(fillet leg)]/2

With the replacement nozzle OD ([ ] as-measured, Reference [13]) and the fillet leg of [ ] (Reference [4]), the corresponding cross-sectional properties of the J-groove weld are summarized in Table 5-3.

Table 5-3: J-groove Weld Cross-Sectional Property

Nozzle OD	R_i, in.	R_o, in.	I, in^4	J, in^4	A, in^2
[ ]	[ ]	[ ]	[ ]	[ ]	[ ]

With the Level D piping loads (Table 5-2) applied to Equations (1) to (5), considering also the pressure load, the SIs on the J-groove weld are calculated, as listed in Table 5-4.

Table 5-4: Stress Intensity on J-groove Weld with Level D Loads (Pressure and Piping Loads)

Nozzle OD	Location	Component stress, psi				Principal stress, psi			SI
		σ_x	σ_y	σ_z	τ_{xy}	σ_1	σ_2	σ_3	psi
[ ]	Inside	[							]
	Outside								
	Mean								

By Table 5-4, with Level D loads and Level A criteria, the highest primary membrane stress intensity is [ ] ksi < S_m (=23.3 ksi), and the highest membrane plus bending stress intensity is [ ] ksi < 1.5S_m (=34.95 ksi). The primary stress requirements for the J-groove weld are satisfied.

For comparison purpose, stress intensities on the J-groove due to the maximum pressure only ([ ] psig Hydrostatic Test pressure) are listed in Table 5-5.

Table 5-5: Stress Intensity on J-groove Weld due to Pressure Only

Nozzle OD	Location	Component stress, psi				Principal stress, psi			SI
		σ_x	σ_y	σ_z	τ_{xy}	σ_1	σ_2	σ_3	psi
[ ]	Inside	[							
	Outside								
	Mean								]

Pure Shear (NB-3227.2)

By Table 5-4, the maximum primary shear stress calculated from the transverse shear forces and the torsional moment across the J-groove weld throat cross-section is [ ] psi, which is less than 0.6S_m (=0.6*23.3=13.98 ksi) the allowable for the average primary shear stress.

In addition, axial forces on the nozzle (and torsional moment as well) may develop shear stresses along the weld interface with the nozzle outside surface. The shear area A_s = [ ] in^2, where [ ] is the as-measured nozzle OD and [ ] is the J-groove depth; weld fillet leg is conservatively not considered. The axial force due to pressure and piping loads is F_v = [ ] lbs, where [ ] psig is the pressure, [ ] is the as-measured J-groove bore ID (max. value) and [ ] lbs is the piping axial load. The shear stress due to axial forces is then F_v/A_s = [ ] psi. Conservatively adding the shear stress above ([ ] psi), the total is [ ] psi ([ ]), which is less than 0.6S_m (=0.6*23.3=13.98 ksi) the allowable for the average primary shear stress.

This requirement is satisfied.

5.1.2.2 New Nozzle

Tentative Pressure Thickness (NB-3324.1)

For the thick portion of the nozzle,

$t = \frac{PR_o}{S_m + 0.5P}$ where R_o is the outside radius of the nozzle, P the Design Pressure ([ ] psi, Reference [9])

The as-measured nozzle OD is [ ] (Reference [13]). With P ([ ] psi), R_o ([ ]) and S_m (23.3 ksi), the tentative pressure thickness is

$$t = \frac{[\quad]psi \times [\quad]in}{23300\ psi + 0.5 \times [\quad]psi} = [\quad]in.$$

The minimum possible nozzle wall thickness considering the nozzle ID tolerances is

[ ]

For the thin portion of the nozzle,

$t = \frac{PR}{S_m - 0.5P}$ where R = [ ] is the inside radius of the nozzle end, P the Design Pressure ([ ] psi)

$$t = \frac{[\quad]psi \times [\quad]in}{23300\ psi - 0.5 \times [\quad]psi} = [\quad]\ in.$$

The nozzle wall thickness of all three sizes at the nozzle thin end is

[ ]

Therefore, the tentative thickness requirement is met.

Stress Intensity (SI)

Stress intensities on the replacement nozzle due to combined loads (pressure, piping loads) are calculated based on the cross-section at the terminal end of the nozzle, with the R_i and R_o as follows. Primary stresses calculated at this location of the nozzle bounds those in other part of the nozzle.

R_i = [ ]

R_o = [ ]

With the Level D piping loads (Table 5-2) applied to Equations (1) to (5), the SIs on the replacement nozzle are calculated, as listed in Table 5-6.

Table 5-6: Stress Intensity on Replacement Nozzle with Level D Loads (Pressure and Piping Loads)

Location	Component stress, psi				Principal stress, psi			SI
	σ_x	σ_y	σ_z	τ_{xy}	σ_1	σ_2	σ_3	psi
Inside	[							]
Outside								
Mean								

By Table 5-6, with Level D loads that are significantly higher than the Level A/B loads, and with Level A criteria, the highest primary membrane stress intensity is [ ] ksi < S_m (=23.3 ksi), and the highest membrane plus bending stress intensity is [ ] ksi < $1.5S_m$ (=34.95 ksi). The primary stress requirements for the replacement nozzle are satisfied.

For comparison purpose, stress intensities on the nozzle due to the maximum pressure only ([ ] psig Hydrostatic Test pressure) are listed in Table 5-7.

Table 5-7: Stress Intensity on Replacement Nozzle due to Pressure Only

Location	Component stress, psi				Principal stress, psi			SI
	σ_x	σ_y	σ_z	τ_{xy}	σ_1	σ_2	σ_3	psi
Inside	[							]
Outside								
Mean								

5.1.2.3 Weld Pad

The cross-section of the weld pad is significantly larger than the J-groove weld cross-section and it is made of an equivalent material. [ ]
The primary stress requirements for the weld pad are satisfied, as the requirements are satisfied for the J-groove weld.

5.1.2.4 Reinforcement Requirements for Openings

NB-3332.1, Reference [2] is used to determine the reinforcement requirements for the 2″ N16A nozzle.

5.1.2.4.1 Methodology

The required parameters used to demonstrate that the N16A nozzle opening does not require reinforcement are determined using NB-3332.1 (a), NB-3332.1 (b) and NB-3332.1 (c), Reference [2] as follows:

1) The repaired nozzle bore diameter, including the corrosion over the remaining service life is compared with the maximum allowable opening diameter determined per NB-3332.1 (a). In addition, the sum of diameters of unreinforced openings within a specified circle is compared with the required parameter per NB-3332.1 (a).
2) The distance between unreinforced openings is compared with the minimum requirement per NB-3332.1 (b).
3) The distance of unreinforced opening to the edge of a locally stressed area is compared with the minimum requirement per NB-3332.1 (c).

5.1.2.4.2 NB-3332.1 (a)

1) A single opening has a diameter not exceeding $0.2\sqrt{Rt} = [$]

where: R is the mean radius, $R = R_i + \frac{t}{2} = [$]

$R_i = [$] is the inside radius to the base metal taken from Reference [9] Part 1 of 5, page 673.

t = [ ] is the nominal thickness of the vessel shell taken from Reference [9] Part 1 of 5, page 696.

The as-measured nozzle bore diameter is [ ] (Reference [13], max. value). The corrosion rate of [ ] inches per year is taken from Reference [10]. Service duration is conservatively considered for [ ] years.
The maximum bore diameter considering corrosion for [ ] years and bore tolerances is therefore [ ] in + ([ ] in/year x [ ] years).

It is concluded that the final bore diameter of [ ] inches is smaller than the maximum diameter allowed for unreinforced openings of [ ]

2) or if there are two or more openings within any circle of diameter $2.5\sqrt{Rt}$ = [ ] but the sum of the diameters of such unreinforced openings shall not exceed $0.25\sqrt{Rt}$ = [ ]

There are no openings within the circle of [ ] inches of diameter assessed based on Reference [9] Part 1 of 5, page 672.

5.1.2.4.3 NB-3332.1 (b)

No two unreinforced openings shall have their centers closer to each other, measured on the inside of the vessel wall, than 1.5 times the sum of their diameters.

The closest unreinforced nozzle per Reference [9], Part 1 of 5, page 672, is another 2″ instrumentation nozzle. By inspection these nozzles are farther apart than 1.5 times the sum of their diameters.

5.1.2.4.4 NB-3332.1 (c)

NB-3332.1(c) requires that no unreinforced opening shall have its center closer than $2.5\sqrt{Rt}$ to the edge of a locally stressed area in the shell. The distance of $2.5\sqrt{Rt}$ was determined to be [ ] Per Reference [9], the only discontinuities within [ ] of the subject opening that could possibly lead to a locally stressed area in the shell are the Jet Pump Riser Support Pads and the Surveillance Specimen Brackets.
However, neither of these discontinuities creates a locally stressed area in the shell. The closest applicable guidance[1] in Table NB-3217-1 is for "Any shell or head, near nozzle or other opening." Based on that guidance, and only considering stresses in the shell (per NB-3332.1(c)), only membrane stress from this discontinuity can possibly be classified as P_L. Bending in the shell is clearly Secondary. Regardless of how much load exists on these pads or brackets, the membrane stress induced in the shell cannot be significant. As already stated, bending in the shell would be classified as Secondary (Q), and any stresses from stress concentrations at the pad or bracket juncture with the shell are clearly Peak stress (F). Since the stresses in these regions are either Q or F, they are not P_L, and this is not a "locally stressed area in the shell." Since there are no locally stressed areas in the shell within [ ] NB-3332.1(c) is satisfied.

[1] It is recognized that this is not an opening, and while there is no direct guidance for an attachment, this is consistent with the clear intent of the Code.

5.1.2.4.5 Conclusion of Reinforcement Requirement for Openings

The above calculation concluded that no reinforcement is required per the 2013 edition of the ASME code, Section NB-3332.1.

5.2 Interference Check

There is a minimum 1/16″ gap between the end of the original nozzle remnant and the replacement nozzle. A conservative calculation will be done to verify that this gap is sufficient to accommodate thermal growth, ΔL.

Interference between the nozzle and the nozzle remnant

Original Nozzle material: [ ]

Nozzle thermal expansion coefficient: α_{noz} = 8.2x10^{-6} in/in/°F (conservatively use Alloy 690 value at 600°F from Reference [8] for [ ])

Nozzle length: L = [ ] (use full thickness of RV base metal and the new wed pad, see Reference [3])

Nozzle temperature: T = [ ] (use highest operating temperature from Reference [6])

$\Delta L = L * \alpha_{noz} * \Delta T$ = [ ]

The nozzle thermal growth of [ ] is less than the minimum gap of [ ] The gap is sufficient to prevent interference.

Interference between the nozzle and the reducing coupling

Reducing coupling material: [ ]

Reducing coupling thermal expansion coefficient: α_{ss} = [ ] in/in/°F (SS at [ ] °F from Reference [8])

Since the SS coupling has a higher thermal expansion coefficient than that of the Alloy 690 (replacement nozzle), the gap is increased at elevated temperatures and no interference is expected.

5.3 Secondary and Peak Stresses

The ASME Code places a limit on secondary stresses in order to prevent failure by excessive distortion caused by the repeated application of loads. The Code also limits peak stresses, through the cumulative fatigue usage factor, in order to prevent failure by fatigue.

The repair weld and replacement nozzle are subject to the same transients as the original design. However, the original weld was on the inside surface of the vessel, while the repair weld is located on the outside surface of the vessel. As compared with the original J-groove weld location, fluid flow rate is significantly lower at the new J-groove weld location, resulting in lower heat transfer at the new J-groove weld. Therefore, the new J-groove weld will experience less severe transient thermal stresses, and the primary plus secondary stress intensity range of the repair weld is no larger than that on the original weld. The P+Q stress range due to piping loads is negligible, as the main contribution to the SI range is due to the pressure load from a comparison of values presented in Table 5-4 and Table 5-5. Secondary stresses due to hole dilation are not significantly different between the original J-groove weld and new J-groove weld. It can be concluded that the single cycle fatigue usage factor for the repair is [ ] of the usage factor as analyzed in Reference [9]. Since the usage factors

in Reference [9] are all within the limit (1.0), there is ample margin to the ASME fatigue criteria for this one cycle justification.

Per Reference [9], the primary plus secondary (P+Q) stress intensity range calculated for the original nozzle exceeded the allowable ($3S_m$); it was then justified through the simplified elastic-plastic analysis. The replacement nozzle end where the reducing coupling is welded has the same dimensions as the original nozzle safe end. The original safe end is made of stainless steel ([ ]), which has the same thermal expansion coefficient as the stainless coupling ([ ]). With the replacement nozzle, the safe end is eliminated and the coupling is directly welded on to the nozzle end. Since the thermal expansion coefficient of the SS coupling is higher than that of the Alloy 690 nozzle, thermal stresses may develop in the nozzle at high temperature when the coupling is fitted in.

The weld connecting the coupling and the nozzle is evaluated in Reference [11] using NB-3600 piping criteria. The P+Q intensity range due to thermal effects is [ ] ksi (Reference [11]). The stresses in this piping analysis were based on coefficients of thermal expansion (CTEs) taken at room temperature, consistent with piping rules. The difference in CTEs between the nozzle and the coupling at room temperature is [ ] However, using vessel rules, the CTEs would be taken at operating temperature. This leads to a CTE difference of [ ] Considering the difference in analysis methodology between NB-3 .e., 1.6/0.8) is used as a conservative estimate of the P+Q SI range from differential thermal growth at the nozzle end. This is a conservative estimate because the piping analysis is required to use the elastic moduli (E) at room temperature, where vessel rules would use E's at operating temperature. Therefore, a conservative estimate for the stress caused by differential thermal growth is [ ] ksi.

With the primary stresses due to pressure and piping loads as calculated in Section 5.1.2.2, the total P+Q SI range at the nozzle end may be estimated to be [ ] ksi, which is less than the allowable $3S_m$ (=3*23.3 = 69.9 ksi).

Considering a factor of [ ] for fatigue evaluation, the magnitude of alternating stress is: S_{alt} = [ ] ksi. By the design fatigue curve in Fig. I-9.2 of Reference [12], the allowable number of cycles is over 700. In addition to the start up and shut down transients, SCRAM (Loss of Feedwater Pumps) and the Post Pressure Test Flushing are the only transients out of Normal/Upset transients that may have some contribution to the fatigue usage, per Report #21 in Reference [9]. At Region B, temperature variation of SCRAM is less than that during start up and shut down. Based on the design number of cycles specified in Reference [5], as the projected number of cycles, it is considered sufficient to consider one start up and shut down cycle plus two other transients for the one cycle operation. To be conservative, [ ] This yields the final fatigue usage factor to be [ ] for the nozzle.

5.4 Corrosion Evaluation

Corrosion effects have been evaluated in Reference [10] and are considered in Section 5.1.2.4 for reinforcement requirements. Corrosion has no impact on the replacement nozzle and new pad.

6.0 COMPUTER USAGE

No specific engineering software is used in this calculation.

7.0 CONCLUSION

The repair of instrumentation nozzle N16A is acceptable for at least one fuel cycle of operation.

8.0 REFERENCES

1. [ ]
2. ASME Boiler and Pressure Vessel Code, Section III, Division 1, 2013 Edition.
3. [ ]
4. [ ]
5. [ ]
6. [ ]
7. ASME B16.11-2016, Forged Fittings, Socket-Welding and Threaded.
8. ASME Boiler and Pressure Vessel Code, Section II, Part D, 2013 Edition.
9. [ ]
10. [ ]
11. [ ]
12. ASME Boiler and Pressure Vessel Code, Section III Appendices, 2013 Edition.
13. [ ]

Attachment 7

"Corrosion Evaluation of the Peach Bottom Unit 2 N16-A Reactor Vessel Nozzle Modification," Document Number 51-9321006–001 (Non-Proprietary Version)

framatome

Framatome Inc.

Engineering Information Record

Document No.: 51 - 9321006 - 001

Corrosion Evaluation of the Peach Bottom Unit 2 N16-A Reactor Vessel Nozzle Modification

Safety Related? ☒ YES ☐ NO

Does this document establish design or technical requirements? ☐ YES ☒ NO

Does this document contain assumptions requiring verification? ☐ YES ☒ NO

Does this document contain Customer Required Format? ☐ YES ☒ NO

Signature Block

Name and Title/Discipline	Signature	P/LP, R/LR, M, A-CRF, A	Date	Pages/Sections Prepared/Reviewed/ Approved or Comments
Roluf Andersen Engineer I Materials Engineering	*RB ANDERSEN 11/14/2020*	P		All
Stacy Yoder Engineer III Materials Engineering	*SL YODER 11/14/2020*	R		All
Ryan Hosler Supervisory Engineer Materials Engineering	*RS HOSLER 11/14/2020*	M		All
Ryan Hosler Supervisory Engineer Materials Engineering	*RS HOSLER 11/14/2020*	A		All

Note: P/LP designates Preparer (P), Lead Preparer (LP)
M designates Mentor (M)
R/LR designates Reviewer (R), Lead Reviewer (LR)
A-CRF designates Project Manager Approver of Customer Required Format (A-CRF)
A designates Approver/RTM – Verification of Reviewer Independence

Project Manager Approval of Customer References (N/A if not applicable)

Name (printed or typed)	Title (printed or typed)	Signature	Date
Alan Stalker	Project Manager	*AR STALKER 11/14/2020*	

Project Manager signature above indicates the applicable IBPE approval of Reference [5].

Record of Revision

Revision No.	Pages/Sections/ Paragraphs Changed	Brief Description / Change Authorization
000	All	Original release (November 2020). The Proprietary version of this document is 51-9320932-000.
001	See Description	Updated per the proprietary version of this document, 51-9320932-001.

Table of Contents

Page

SIGNATURE BLOCK 2
RECORD OF REVISION 3
LIST OF FIGURES 5
1.0 PURPOSE 6
2.0 ASSUMPTIONS 9
2.1 Assumptions Requiring Verification 9
2.2 Justified Assumptions 9
3.0 CORROSION OF EXPOSED LOW ALLOY STEEL 9
3.1 General Corrosion 9
3.2 Galvanic Corrosion 10
3.3 Crevice Corrosion 10
3.4 Stress Corrosion Cracking 10
4.0 CORROSION OF ALLOY 690 AND ALLOY 52M 13
5.0 CONCLUSION 13
6.0 REFERENCES 14

List of Figures

Page

Figure 1-1: Original Configuration (Shown with Sealing Plug in Place) [1] [2] 7

Figure 1-2: Final Repair Configuration (Shown with Sealing Plug in Place) [1] [2] 8

Figure 3-1: [ ] 12

1.0 PURPOSE

The repair of the N16-A reactor vessel nozzle in the Peach Bottom Unit 2 reactor vessel will change the penetration configuration in the following ways: 1) the repair exposes the low alloy steel (LAS) reactor vessel to water conditions, 2) the repair includes a new Alloy 690 nozzle as part of the pressure boundary, and 3) the repair includes a new Alloy 52M weld pad and partial penetration J-groove weld as part of the pressure boundary [1] [2]. Also, the reducing coupling to nozzle weld is now an Alloy 52M dissimilar metal weld. The original configuration and the final repair configuration, as well as materials, are shown in Figure 1-1 and Figure 1-2 respectively.

The following corrosion evaluation considers potential material degradation due to each of these changes. Information contained in bold brackets in this document is considered Proprietary to Framatome.

Figure 1-1: Original Configuration (Shown with Sealing Plug in Place) [1] [2]

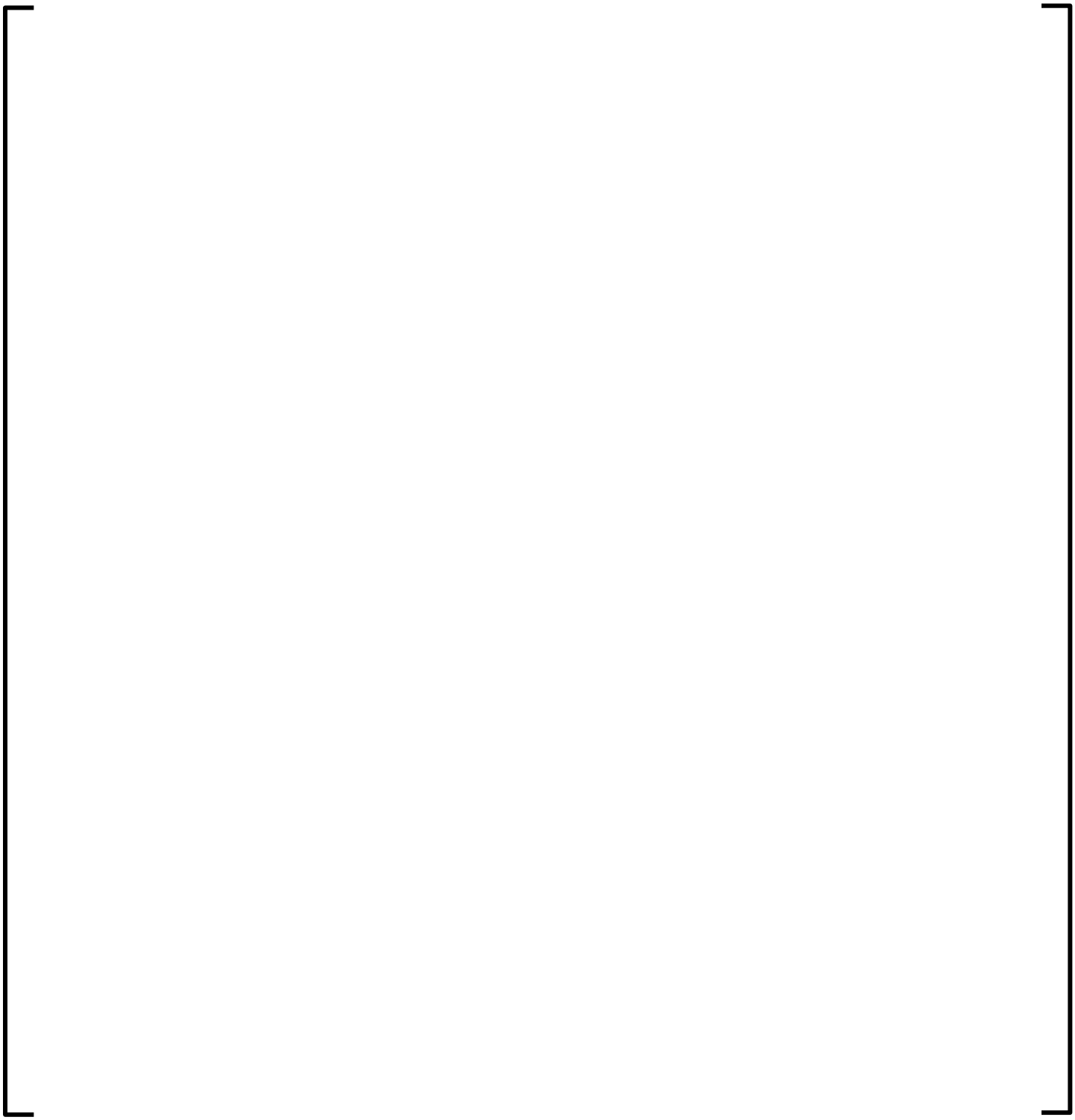

Figure 1-2: Final Repair Configuration (Shown with Sealing Plug in Place) [1] [2]

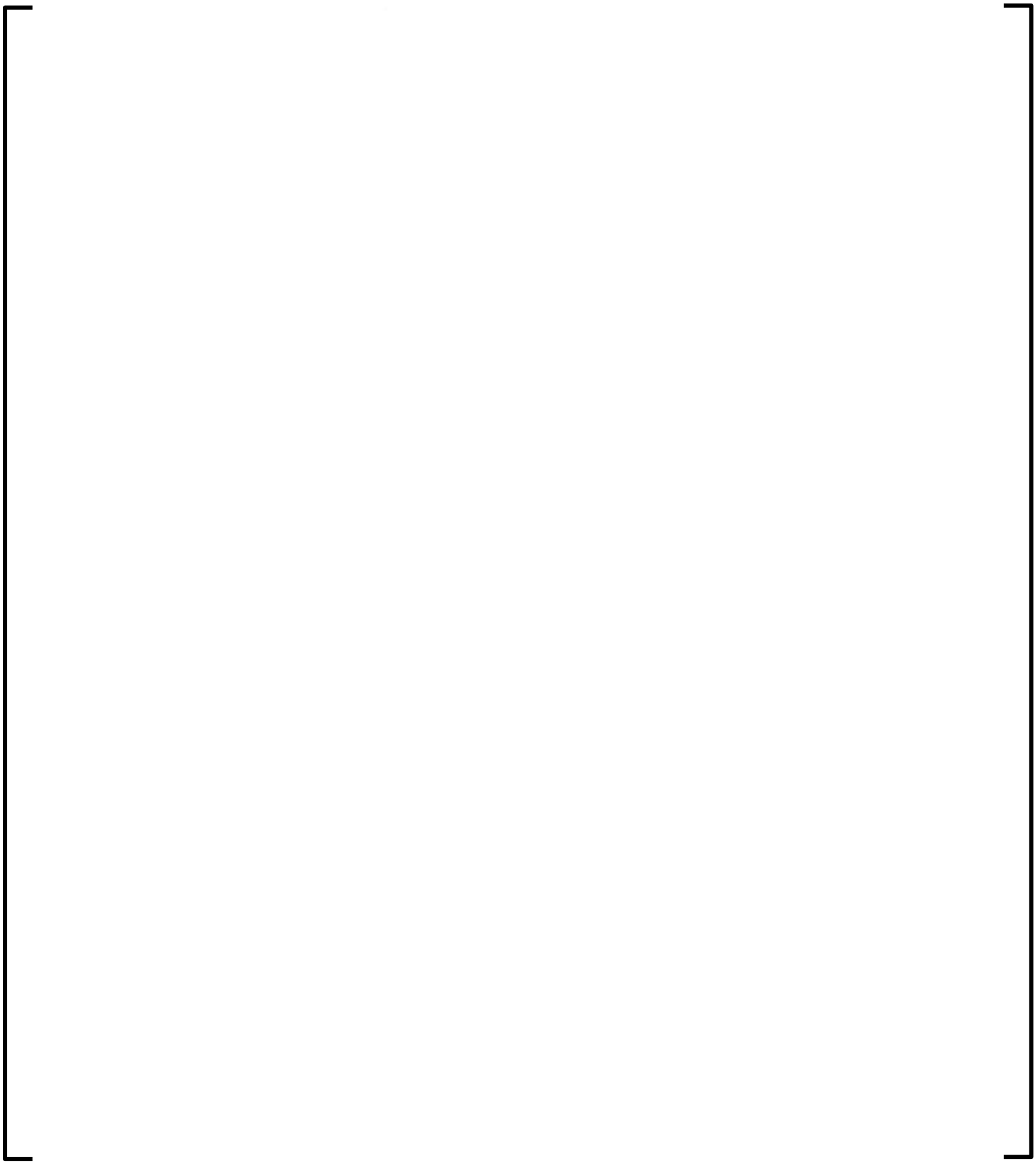

2.0 ASSUMPTIONS

2.1 Assumptions Requiring Verification

[ ]

2.2 Justified Assumptions

[

]

3.0 CORROSION OF EXPOSED LOW ALLOY STEEL

The LAS reactor vessel material exposed due to the repair, as shown in red in Figure 1-2, will be in the water space environment given the elevation of the N16-A nozzle [1]. The requirements of the Reactor Water Chemistry control program for Peach Bottom are based on BWRVIP-190, Revision 1 [3] [4].

3.1 General Corrosion

Due to the repair configuration, a small portion of the LAS reactor vessel material will be openly exposed to boiling water reactor (BWR) water and, thus, general corrosion is considered. [

]

[

]

3.2 Galvanic Corrosion

3.3 Crevice Corrosion

[ ] The environmental conditions in a crevice can become aggressive with time and can cause accelerated local corrosion.

3.4 Stress Corrosion Cracking

Although it is very unlikely that SCC cracks will initiate and propagate in LAS under normal BWR conditions, it is impossible to completely rule out. Hence, it is prudent to examine the feasibility of performing an allowable flaw evaluation for an assumed flaw propagating from the J-groove weld into the LAS by applying the American Society of Mechanical Engineers (ASME) Boiler and Pressure Vessel (B&PV) Code Section XI criteria [10].

[ ]

- As noted in Section 3.0, requirements of the Reactor Water Chemistry control program for Peach Bottom are based on BWRVIP-190, Revision 1. See Section 2.2 for Justified Assumption 1 for additional details regarding [ ]

[

]

Figure 3-1: [

]

[

]

This CGR equation/curve was used to support the ASME Section XI analysis [13], which concluded that the postulated flaw is acceptable for one cycle of operation.

4.0 CORROSION OF ALLOY 690 AND ALLOY 52M

Stress corrosion cracking failures of Alloy 600 and its associated weld metals (Alloy 82/182) have occurred in domestic and international light water reactors. The BWR industry addressed this issue by replacing or modifying affected materials with a modified version of Alloy 600 and Alloy 82/182 [14]. The modified Alloy 82/182 added carbide stabilizers (niobium and tantalum) to minimize chromium depletion at the grain boundaries. The pressurized water reactor (PWR) industry selected Alloy 690 and Alloy 52/152 as replacement materials [15]. Alloy 690 was also thermally treated to improve the microstructure, but grain boundary chromium depletion of Alloy 690/52/152 was avoided by doubling the chromium content (from ~15% to ~30%) instead of using carbide stabilizers. Laboratory studies indicate that Alloy 690 and Alloy 52/152 have superior SCC resistance relative to the non-modified Alloy 600 and Alloy 82/182 [15].

Although most testing of Alloy 690/52/152 has been under PWR conditions, some studies have been performed in environments more similar to BWRs. Creviced U-bend specimens of Alloy 600 and Alloy 690 were tested at 600°F for 48 weeks with an environment of 6 ppm oxygen [16]. The Alloy 600 readily cracked, whereas Alloy 690 showed no cracking. Also, testing of Alloy 690 in high purity water containing 36 ppm oxygen at 289°C (~550°F) for 47 weeks resulted in no cracking [16].

Extensive testing has been performed on Alloy 52/152 in high temperature deaerated water, which indicate that Alloy 52/152 is much less susceptible to SCC compared to Alloy 82/182 (the Alloy 600 weld metal) [15] [17] [18]. Test data of Alloy 52/152 in a high temperature oxygenated environment is not readily available, but Alloy 52/152 is expected to have a low susceptibility to SCC under these conditions as well based on the similarity of Alloy 52/152 to Alloy 690.

The only difference between the Alloy 52M to be used in the repair and Alloy 52/152 are small alloying additions to improve weldability. The corrosion resistance is expected to be similar. Based on laboratory studies and operating experience, the replacement higher chromium content nickel-based alloys (Alloy 690 and Alloy 52M) are much less susceptible to SCC than Alloy 600 and Alloy 182 and SCC of these materials is not expected during the life of the modification.

5.0 CONCLUSION

The modification of the N16-A reactor vessel nozzle at Peach Bottom exposes the LAS reactor vessel in a small area to a water environment and introduces new materials (Alloy 690 and Alloy 52M). For the exposed LAS, general corrosion, galvanic corrosion, crevice corrosion, and SCC were evaluated. It is concluded that 1) galvanic corrosion and crevice corrosion are bound by general corrosion, 2) the projected material loss by general corrosion is not a concern for one fuel cycle based on the Section III analysis, and 3) SCC is not a concern for one fuel cycle based on the Section XI analysis. In addition, it is concluded that SCC of the replacement higher chromium content nickel-based alloys (Alloy 690 and Alloy 52M) is not a concern over the life of the modification.

6.0 REFERENCES

References identified with an (*) are maintained within Exelon Records System and are not retrievable from Framatome Records Management. These are acceptable references per Framatome Administrative Procedure 0402-01, Attachment 7. See page 2 for Project Manager Approval of customer references.

1. [ ]
2. [ ]
3. *BWRVIP-190 Revision 1: BWR Vessel and Internals Project, Volume 2: BWR Water Chemistry Guidelines - Technical Basis. EPRI, Palo Alto, CA: 2014. 3002002623.
4. [ ]
5. [ ]
6. [ ]
7. ASM Handbook, Volume 13, "Corrosion", Formerly 9th Edition, Metals Handbook.
8. D.C. Vreeland, et al., "Corrosion of Carbon and Low-Alloy Steels in Out-of-Pile Boiling-Water-Reactor Environment," Corrosion, Vol 17, No. 6, 1961.
9. [ ]
10. ASME B&PV Code, Section XI, Rules for Inservice Inspection of Nuclear Power Plant Components, Division 1, 2013 Edition, Subject to the conditions of 10 CFR 50.55a.
11. [ ]
12. [ ]
13. [ ]
14. NUREG/CR-6923, "Expert Panel Report on Proactive Materials Degradation Assessment."
15. Materials Reliability Program (MRP): Resistance to Primary Water Stress Corrosion Cracking of Alloys 690, 52, and 152 in Pressurized Water Reactors (MRP-111). EPRI, Palo Alto, CA: 2004. 1009801.

16. Sedriks, A.J., Schultz, J.W., Cordovi, M.A., "Inconel Alloy 690 – A New Corrosion Resistant Material," Corrosion Engineering (Boshoku Gijutsu), vol. 28, pp. 82-95, 1979, Japan Society of Corrosion Engineering.

17. M. J. Psaila-Dombrowski et al., "Evaluation of Weld Metals 82, 152, 52 and Alloy 690 Stress Corrosion Cracking and Corrosion Fatigue Susceptibility," Eighth International Symposium on Environmental Degradation of Materials In Nuclear Power Systems – Water Reactors, Aug 10-14 1997, Amelia Island, FL, ANS.

18. Crum, J.R., Nagashima, T., "Review of Alloy 690 Steam Generator Studies," Eight International Symposium on Environmental Degradation of Materials In Nuclear Power Systems – Water Reactors, Aug 10-14 1997, Amelia Island, FL, ANS.